

MASTER OF SCIENCE  
IN PETROLEUM ENGINEERING

OPTIMIZATION OF PETROLEUM  
PRODUCTION UNDER INDUSTRIAL  
CONSTRAINTS USING ALTERNATIVE  
OBJECTIVE FUNCTIONS AND ADJOINT  
GRADIENT-BASED TECHNIQUES

MASTER THESIS

**CHRISTINI FANDRIDI**  
Technical University of Crete  
Department of Mineral Resources Engineering

Chania 15 January 2017



PRINCIPAL ADVISOR: Dr. Drosos Kourounis

EXAMINATION COMMITTEE

Prof. Vassileios Gaganis

Prof. Dionysios Hristopoulos

Dr. Drosos Kourounis



*To my family*



# Contents

<b>1</b>	<b>Oil production methods</b>	<b>1</b>
1.1	Oil production methods	2
1.2	Primary recovery	2
1.3	Secondary recovery	3
1.4	Enhanced oil recovery	4
1.4.1	Thermal techniques	4
1.4.2	Non thermal techniques	5
1.4.3	Nitrogen Injection	6
1.5	Need for simulation and optimization	8
1.6	Previous work	9
1.7	The scope of this work	10
<b>2</b>	<b>Production Optimization</b>	<b>11</b>
2.1	Gradient-free methods	11
2.1.1	Genetic algorithms (GAS)	11
2.1.2	Particle Swarm Optimization(PSO)	12
2.2	Gradient-based methods	12
2.2.1	Sequential quadratic programming (SQP)	12
2.2.2	Interior point optimization (IPO)	13
2.3	Oil-gas compositional simulation equations	14
2.4	Adjoint equations for the compositional system	15
2.4.1	Automatic differentiation	15
2.4.2	Discrete adjoint formulation	16
2.4.3	Continuous adjoint formulation	18
2.4.4	Continuous versus discrete adjoint formulation	20
2.4.5	Solution of adjoint equations	21
2.5	Gradient-based optimization and related software	22

**3 Benchmark Problems 25**

- 3.1 Example 1 -  $\Pi$  obstacle 27
  - 3.1.1 Optimization of cumulative oil 29
  - 3.1.2 Optimization with geological continuation 32
- 3.2 Example 2 - Top layer of SPE 10 model 37
  - 3.2.1 Optimization of cumulative oil 39
  - 3.2.2 Optimization with geological continuation 43
  - 3.2.3 Alternative objectives 50
- 3.3 Concluding remarks 52

**Bibliography 55**

# Abstract

The optimization of oil production is a tedious and computationally intensive process that requires the solution of time dependent nonlinear set of partial differential equations describing the flow of hydrocarbons in anisotropic porous media. Optimization of production is usually performed using either gradient free techniques like genetic algorithms, particle swarm algorithms, or gradient-based techniques where the gradients are computed through the solution of the adjoint problem. A gradient-based optimization method, in which the gradient is computed using an adjoint formulation, is often the method of choice since in contrast to numerical perturbation techniques that require as many objective function evaluations as the number of control parameters, the gradient using adjoint-based techniques is obtained only at a small fraction of the time spent for the evaluation of the objective function. It is well known that for non-convex optimisation problems, gradient-based techniques are likely to get trapped in poor local optima. A common practise is to launch several independent optimisation runs from different initial guesses or to combine ideas from gradient-free algorithms with gradient-based to benefit from the merits of both. An adequate sampling of the search space would require an intractable number of simulations and it is thus impossible.

The aim of this work is to exploit an observation in homogeneous reservoirs, where the global optimum, when optimising cumulative oil recovery, is usually achieved from practically any initial guess. This observation suggest to optimize cumulative oil by adopting a “geology continuation” method. In this novel approach the porosity and permeability fields, gradually switch from some average homogeneous values chosen heuristically for the particular benchmark, to the inhomogeneous geological properties characterizing the reservoir. The optimal controls from each step become the initial controls to the next step.

In addition instead of maximizing the cumulative oil we suggest to minimize modified versions of the residual oil function which are likely to be more convex and thus less likely to lead in poor local optima.



# Chapter 1

## Oil production methods

### Need for energy

Modern industrial societies consume large quantities of energy in order to maintain today's high standard of living. Most of that energy comes as a result of the technology of oil production. According to the U.S. Energy Information Administration's (EIA) International Energy Outlook 2016, the global supply of crude oil, other liquid hydrocarbons, and biofuels is expected to be adequate to meet the world's demand for liquid fuels through 2040. There is substantial uncertainty about the levels of future liquid fuels supply and demand. According to current prognosis, oil production in matured reservoirs is expected to decline and this could create a gap between supply and demand of hydrocarbons in various parts of the world. To counteract this growing demand-supply discrepancy, the petroleum industry will have to give more attention to their mature fields to sustain current production levels. It should be realized that most operators have not exploited the full capacity of mature fields to their potential. In addition to this they face the challenge of developing green fields in such a way that they can be produced to their maximum potential in the future. With a mean recovery factor of about 36%, there is an immense opportunity for "production optimization".

The primary objective within reservoir management is to provide optimal production scenarios, accompanied by estimates of expected hydrocarbon recovery, ultimately resulting in an optimized field development plan. Elements of such a plan include recovery techniques, well types and position or pattern designs, completion types, and production scheduling. In fields with significant complexity, automated workflows based on numerical algorithms will need to be used to find optimal choices for all these variables.

## 1.1 Oil production methods

During the life of a producing oil field, several production stages are encountered. Initially, when a field is brought into production, oil flows naturally to the surface due to current reservoir pressure in the primary stage. As reservoir pressure drops, water is typically injected to boost the pressure, so that it displaces the oil in the so called “secondary” stage. Lastly, the remaining oil can be recovered by a variety of methods such as CO<sub>2</sub> injection, natural gas miscible injection, and steam recovery in a tertiary or enhanced oil recovery (EOR) phase [Meyer, 2007].

## 1.2 Primary recovery

Glover [Glover, 2001] explained all recovery methods, including primary recovery mechanism as it is the stage when the natural energy of the reservoir is used to transport hydrocarbons towards and out of the production wells. The earliest possible determination of the drive mechanism is a primary goal in the early life of the reservoir, as its knowledge can greatly improve the management and recovery of reserves from the reservoir in its middle and later life. There are five important drive mechanisms: (i) Solution gas drive; (ii) Gas cap drive; (iii) Water drive; (iv) Gravity drainage; (v) Combination or mixed drive. All these mechanisms maintain the reservoir pressure, though water drive maintains much higher pressure than the gas drive mechanisms (Figure 1.2).

### Solution gas drive

In solution gas drive, the expansion of the dissolved gases in the oil and water provides most of the reservoirs drive energy. Oil recovery from this type is typically between 20% and 30% of original oil in place.

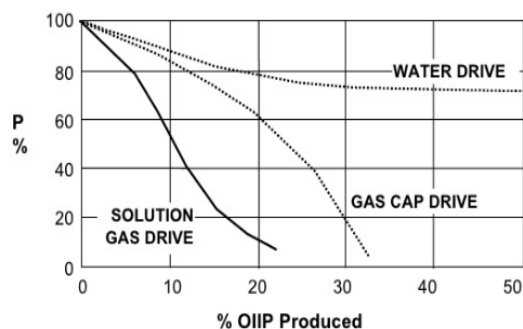


Figure 1.1: Pressure trends under various drive mechanisms.

**Gas cap drive**

As production continues, the gas cap expands pushing the gas-oil contact (GOC) downwards. Eventually the GOC will reach the production wells and the gas oil ratio (GOR) will increase by large amounts. The recovery of gas cap reservoirs can be (20% to 40% OOIP).

**Water drive**

The drive energy is provided by an aquifer that interfaces with the oil in the reservoir at the oil-water contact (OWC). The recovery from water driven reservoirs is usually good (20-60% OOIP).

**Gravity drainage**

Gravity drainage is the fourth drive force that might be considered for drive mechanism where the density differences between oil and gas and water result in their natural segregation in the reservoir. This process is relatively weak and in practice is only used in combination with other drive mechanisms.

## 1.3 Secondary recovery

After initial discover and production, typical oil reservoirs lose the drive mechanism of gas or water that originally forced the oil to the surface. The second stage of hydrocarbon production in which an external fluid such as water: usually named water flooding or water injection or gas: referred to as gas flooding or gas injection, is injected into the reservoir through injection wells. By secondary recovery methods, another 15-20% may be produced. [Fleshman and Lekic, 1999].

**Water flooding**

Water Flooding is implemented by injecting water into a set of wells while producing from the surrounding wells. Water flooding projects are generally implemented to accomplish reservoir pressure maintenance and as a water drive to displace oil from the injector wells to the producer wells[Fleshman and Lekic, 1999].

**Gas flooding**

This method is similar to water flooding in principal, and is used to maintain gas cap pressure even if oil displacement is not required. Usually the produced natural gas is re-injected to the reservoir in order to maintain reservoir pressure rather than to displace the hydrocarbon.

## 4 · OIL PRODUCTION METHODS

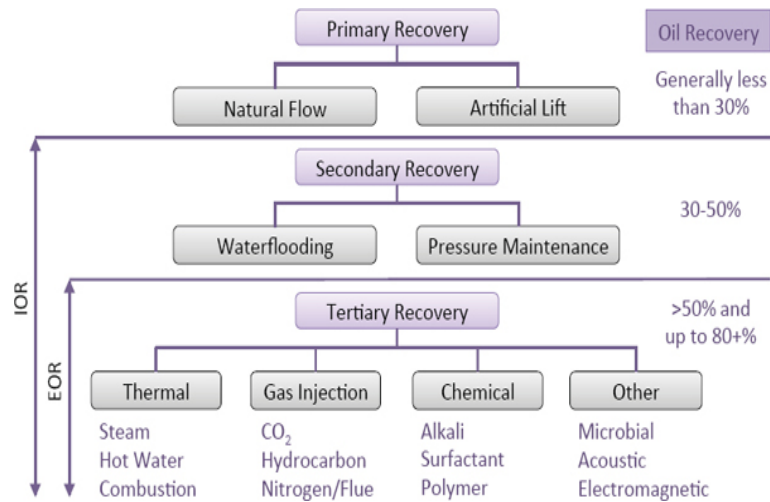


Figure 1.2: The different oil recovery stages and the corresponding oil recovery factor.

### 1.4 Enhanced oil recovery

Enhanced oil recovery techniques refer to the recovery of oil through the injection of fluids and energy not normally present in the reservoir [Romero-Zeran, 2012]. The objectives of the injected fluids are to achieve mainly two purposes; First is to boost the natural energy in the reservoir; second is to interact with the reservoir rock/oil system to create conditions favourable for residual oil recovery that leads to reduce the interfacial tension between the displacing fluid and oil, increase the capillary number, reduce capillary forces, increase the drive water viscosity, provide mobility-control, create oil swelling, reduce oil viscosity, alter the wettability of reservoir rock [Romero-Zeran, 2012]. Enhanced oil recovery can be divided into two: thermal and non-thermal recovery [Anazi, 2007]. Fig. 2 illustrates oil recovery stages by the different EOR techniques.

#### 1.4.1 Thermal techniques

Thermal methods raise the temperature of the reservoir to heat the crude oil in the formation and therefore reduce its viscosity and/or vaporise part of the oil and thereby decrease the mobility ratio. The increase in heat reduces the surface tension, increases the permeability of the oil and improves the reservoir seepage conditions. The heated oil may also vaporise and then condense to be produced. This operation, however, requires substantial investment in special equipment.

**In-situ combustion (ISC)**

In-situ combustion or fire flooding is a process in which an oxygen containing gas is injected into a reservoir where it reacts with the oil contained within the pore space to create a high temperature self-sustaining combustion front that is propagated through the reservoir.

**Steam Injection**

Steam is injected into the reservoir either continuously or in cycles. Steam floods are easier to control than in-situ combustion. For the same pattern size, the response time is 25-50% lower than the response time for additional production by in-situ combustion [et al., 2010].

**Hot water flooding**

Water-flooding in heavy oils is generally not an efficient way of production due to high viscosity of heavy oil compared to water. In hot water-flooding, thermal energy will increase oil mobility, and possibly improve sweep efficiency [Kermen, 2011].

**1.4.2 Non thermal techniques****Chemical Flooding**

These processes use chemicals added to water in the injected fluid of a water flood to alter the flood efficiency in such a way as to improve oil recovery by: (i) Increasing water viscosity (polymer floods) (ii) Decreasing the relative permeability to water (cross-linked polymer floods) (iii) Increasing the relative permeability to oil (micellar and alkaline floods) [Glover, 2001]

**Polymer flooding**

Polymers improve both vertical and areal sweep efficiency by reducing water-oil ratio. Polymers are injected through water injection wells in order to displace the residual oil. Increasing the displacing fluids viscosity and lowering its relative permeability through plugging [Anazi, 2007].

**Micellar polymer flooding**

It is well known that water and oil cannot be mixed until the third component, surfactant or soap, is added to reduce the interfacial tension between oil and water. Since micellar solution makes fluids miscible in the reservoir, almost 100% of oil can be displaced especially in the presence of alkaline. However, due to reservoir rock non-uniformity in the field, the amount of oil recovered is reduced.

### **Alkaline-surfactant-polymer (ASP) flooding**

During waterflooding residual oil is trapped due to low water viscosity and high water-oil interfacial tension, therefore another way is to inject the three chemicals; alkaline to minimize surface adsorption; surfactant to lower interfacial tension and stabilizes the emulsion. On the other hand, polymer is used to increase viscosity and to improve mobility control and sweep efficiency [et al., 2011].

### **1.4.3 Nitrogen Injection**

Nitrogen itself is an inert gas that gets miscible at very high pressure and efficiently reduces the oil viscosity while providing efficient miscible displacement [Syed et al., 2011]. Nitrogen can be used for the following enhanced oil recovery applications:

#### **Nitrogen immiscible flooding**

Gas is being injected into the crest of the structure to maintain the pressure, to recover the hydrocarbon liquids in the gas cap, and to stabilize the gas/oil contact.

#### **Nitrogen miscibility displacement mechanism**

There are three types of miscibility including; First contact miscibility; Multi- contact miscibility; Vaporizing mass-transfer miscibility [Shine and Holtz, 2008].

#### **Multi-contact miscibility**

This type of miscibility is subdivided into vaporizing gas drive, condensing gas drive [Juttner, 1997].

#### **Gas Flooding Injection**

Gas is generally injected single or intermittently with water and this manner of injection called Water-Alternating-Gas (WAG), has become widely practiced over all of worlds oil fields [Kulkarni, 2003]. According to miscibility between gas injected and oil displaced, gas injection can be classified into two major types: miscible gas injection and immiscible gas injection. In miscible gas injection, the gas is injected at or above minimum miscibility pressure (MMP) which causes the gas to be miscible in the oil. In contrast in immiscible gas injection, flooding by the gas is conducted below MMP. This low pressure injection of gas is used to maintain reservoir pressure to prevent production cut-off and thereby increase the rate of production [Anazi, 2007]. In miscible flooding, the incremental oil recovery is obtained by one of the three mechanisms: oil displacement by solvent

through the generation of miscibility (i.e. zero interfacial tension between oil and solvent hence infinite capillary number), oil swelling, and reduction in oil viscosity [Kulkarni, 2003]. Miscible fluids are 100% soluble in each other. The interfacial tension between miscible fluids is zero. Injection gases include:

### **LPG injection**

Miscible LPG products such as ethane, propane, or butane have first contact miscibility, which means they will be miscible from the first contact with oil. However, LPGs are in such demand as marketable commodity that their use in EOR is limited [Romero-Zeran, 2012]. In particular, this process uses a slug of propane or other liquified petroleum gas (2 to 5% of pore volume PV) followed by natural gas, inert gas, and/or water. Thus, the solvent will bank oil and water ahead, and fully displace all contacted oil [Anazi, 2007].

### **Enriched gas miscible process**

In this process, a slug of methane ( $C_1$ ) enriched with ethane ( $C_2$ ), propane ( $C_3$ ), or butane ( $C_4$ ) (10% to 20% of the PV) and followed by lean gas and/or water is injected from water injection well into the reservoir. When the injected gas contacts virgin reservoir oil,  $C_1$ - $C_3$  are quenched from the injected gas and absorbed into the oil [Anazi, 2007]. The injected HC solvent is usually displaced with cheaper chase leaner or inert gas like Methane or Nitrogen. At reservoir conditions the most usual problem occurs with the hydrocarbon miscible flood is the gravity over-ride because of its lighter density than the oil and water. So that in any miscible flood the Minimum Miscibility Pressure (MMP) plays the most major role to overcome this problem. As a remedial factor the solvent is to be injected at or above the MMP of the reservoir fluid. Once it becomes miscible then it improves the sweep efficiency and fallouts in optimum recovery [Syed et al., 2011].

### **Carbon dioxide ( $CO_2$ ) injection**

Is one of the most proven of these methods. Almost pure  $CO_2$  (>95% of the overall composition) has the property of mixing with the oil to swell it, make it lighter, detach it from the rock surfaces, and causing the oil to flow more freely within the reservoir so that it can be swept up in the flow from injector well to producer well [Melzer and Midland, 2012]. Flooding a reservoir with  $CO_2$  can occur either miscibility or immiscibly. Miscible  $CO_2$  displacement is only achieved under a specific combination of conditions, which are set by four variables: reservoir temperature, reservoir pressure, injected gas composition, and oil chemical composition. From a fundamental point of view,  $CO_2$  EOR works on a very simple principle, namely, that given the right physical conditions,  $CO_2$  will mix miscibly with

oil, acting much like a thinning agent, the same way that gasoline does with motor oil. After miscible mixing, the fluid is displaced by a chase phase, typically water [Meyer, 2007]. In this thesis CO<sub>2</sub> injection as EOR method is going to be examined.

## 1.5 Need for simulation and optimization

Use of reservoir simulation has grown because of its ability to predict the future performance of oil and gas reservoirs over a wide range of operating conditions. Reservoir simulators use numerical methods and high-speed computers to model multidimensional fluid flow in reservoir rock. Technology improvements have enabled a widespread use of integrated simulation models for a better asset management to be fully combined with measured field data. Reliable simulators and adequate computing capacity are available to most reservoir engineers, so simulation is usually practical for all reservoir sizes and all types of reservoir performance studies. Although the use of simulation frequently is optional, it may be the only reliable way to predict the performance of a large, complex reservoir, especially if such external considerations as government regulations influence the production schedule. Even for small reservoirs where simple calculations or extrapolations may be adequate, simulation is often faster, cheaper, and more reliable than alternative methods for predicting performance.[Mattax and Dalton, 1990]

In petroleum fields, hydrocarbon production is often constrained by reservoir conditions, deliverability of the pipeline network, fluid handling capacity of surface facilities, safety and economic considerations, or a combination of these considerations. Optimization of reservoir development requires many evaluations of the possible combinations of the decision variables in order to obtain the best economical strategies. The objective of dynamic production optimization is to find the best operational settings at a given time, subject to all constraints, this gives you greater production gains for longer. Overall, optimization delivers a faster return on investment during initial production, yields greater revenues during plateau and decline, and delays well abandonment. Given the fact that oil prices continue to drop to their lowest levels in several years, oil industry will inevitably turn to optimization in order to continue to deliver the dividend levels that investors have come to expect. Production optimization is no longer an option it is a necessity.

## 1.6 Previous work

In petroleum industry, optimization methods are necessary for history matching, where we adjust the physical properties of the reservoir model, and for optimization of production, where the objective is to maximize either the net present value or the cumulative production of hydrocarbons. All the above methods can be implemented both with gradient-free and gradient-based techniques. Generally, gradient-free techniques are not necessarily guaranteed to find the true global optimal solution, they converge very slowly and require high performance computing infrastructures. On the other hand, for gradient-based techniques, once the gradient is computed there are several options for finding an optimum. Furthermore, proper exploitation of gradient information can significantly enhance the speed of convergence in comparison with a method that does not compute gradients. Another feature of gradient-based methods is that they provide a clear convergence criterion.

Among gradient-based algorithms we consider only the adjoint approach for compositional reservoir simulation problems. Procedures of this type entail the application of optimal control theory and have their roots in the calculus of variations [Bryson and Ho, 2001; Stengel, 1986]. Adjoint-based optimization techniques have been used in a reservoir simulation setting both for history matching (see, e.g., [Chavent et al., 1975; Chen et al., 1974; Li et al., 2003; Oliver et al., 2008; Sarma et al., 2006]) and for production optimization. Much of the early work on their use for optimization of oil recovery was performed by Ramirez and coworkers, who considered the optimization of several different enhanced oil recovery (EOR) processes [Liu et al., 1993; Mehos and Ramirez, 1989; Ramirez, 1987]. In subsequent work, the focus was on gradient-based optimization (and in some cases on the optimization of ‘smart wells’) for water flooding [Asheim, 1988; Brouwer and Jansen, 2004; Sarma et al., 2006; Sudaryanto and Yortsos, 2000; Virnovski, 1991]. Refer to [Jansen, 2011] for a more complete overview of adjoint-based optimization methods. We note additionally that, although not considered here, derivative-free methods can also be applied for production optimization problems – see [Echeverría Ciaurri et al., 2011] for discussion and examples. Recently an adjoint treatment for multicomponent oil-gas compositional systems was presented in [Kourounis et al., 2014]. The formulation included an extensive discussion on engineering constraints that should usually be taken into account in realistic scenarios. These constraints appear either as bounds (box constraints) on the control variables or as inequality constraints on nonlinear functions of the controls and states of the underlying PDEs. Two treatments were proposed for the nondifferentiable constraints: a formal treatment within the optimizer performing lumping for all wells and time steps, and a heuristic approach, where

bound constraints are treated in the optimization and nondifferentiable constraints are satisfied in the forward model. The investigation showed that although standard lumping techniques perform well for simple academic problems, they fail to obtain optimal solutions better than the reference for realistic problems. That result motivated further developments of formal constraint-handling techniques. In [Kourounis and Schenk, 2015] the author introduces a new formal treatment for the nondifferentiable constraints where lumping is avoided to allow for a more realistic discretization of the nonlinear constraints. The performance of the new approach is compared to the ones introduced in [Kourounis et al., 2014] for several different examples of increased complexity.

## **1.7 The scope of this work**

Optimization using gradients converges much faster than gradient-free techniques resulting in significant saving in computational time but it usually gets trapped to poor local optima [Kourounis et al., 2014; Kourounis and Schenk, 2015].

The aim of this work is to exploit an observation in homogeneous reservoirs, where the global optimum, when optimising cumulative oil recovery, is usually achieved from any initial guess. We perform continuation with respect to a parameter that transforms the homogenous reservoir with respect to porosity and permeability, gradually to the original inhomogeneous one, solving an optimal control problem for each distinct value of the parameter. This approach allows us to follow the optimal solution (cumulative oil recovery) as the geology switches from homogeneous to inhomogeneous. This novel technique is presented at the best of our knowledge for first time for production optimization problems and tested in several examples of increased complexity.

# Chapter 2

## Production Optimization

The optimization of oil production is a tedious and computational intensive process that requires the solution of time dependent nonlinear set of partial differential equations describing the flow of hydrocarbons in anisotropic porous media. The optimization of time-varying well settings, such as injection rates, production rates or bottom-hole pressures, is an important aspect of optimal reservoir management. Optimization of production is usually performed using either gradient free techniques like genetic, particle swarm algorithms, or gradient-based techniques where the gradients are computed through the solution of the adjoint problem.

### 2.1 Gradient-free methods

In this section we review the basic gradient-free method employed in industry and academia for the solution of several optimal control problems of the oil industry.

#### 2.1.1 Genetic algorithms (GAS)

Genetic algorithms are commonly used to generate high-quality solutions to optimization and search problems by relying on bio-inspired operators such as mutation, crossover and selection. The method is a general one, capable of being applied to an extremely wide range of problems. Genetic algorithms are based on three essential components:

- Survival of the fittest (Selection).

- Reproduction processes where genetic traits are propagated (Crossover).
- Variation (Mutation).

### **2.1.2 Particle Swarm Optimization(PSO)**

Particle swarm optimization (PSO) is a stochastic, population-based computer algorithm. It applies the concept of swarm intelligence (SI) to problem solving. Swarm intelligence is the property of a system whereby the collective behaviors of (unsophisticated) agents interacting locally with their environment cause coherent functional global patterns to emerge (e.g. self-organization, emergent behavior). Gradient-free methods are not necessarily guaranteed to find the true global optimal solutions, but they are able to find many good solutions.

## **2.2 Gradient-based methods**

Gradient-based optimization methods offer the advantage to construct additional information about the shape of the surface for the particular problem. Hence, the gradient of a function provides information about the behavior of a function such as steepness and extrema in the parameter space. The gradients are computed through the solution of the adjoint problem. With this additional information, the convergence of the search algorithm can be drastically enhanced.

### **2.2.1 Sequential quadratic programming (SQP)**

Sequential quadratic programming (SQP) is an iterative procedure that utilizes a 2.order approximation of the Lagrangian function of a problem. The quadratic formulation of the problem is a local approximation of the real problem and consists of a quadratic objective function and linear equality and/or inequality constraints. SQP can be used both within a trust-region and a line search framework. In a line search framework, the algorithm proceeds by first calculating a search direction. If we are trying to maximize the original problem, a function is then solved that maximize the quadratic approximation in the search direction. When a new iteration point in the direction that was searched has been reached, a new local approximation is constructed and the algorithm proceeds to the next iteration given that a set of optimality conditions has not been fulfilled. SQP is a generalization of Newtons method for unconstrained problems as it uses a quadratic approximation of the Lagrangian function, steps in a direction it believes the optimum lies,

and then creates a new approximation of the original model when a new iteration point has been reached. The main difference between Newton's method and SQP is that for constrained nonlinear problems the Taylor approximation of the original problem cannot be used, as the model problem also needs to incorporate the constraints of the original problem. Instead, the Lagrangian function is used and the constraints of the problem thereby taken into account. SQP is appropriate for small and large problems and it is well-suited to solving problems with significant nonlinearities [Bonnans et al., 2006].

### 2.2.2 Interior point optimization (IPO)

An interior point method is a linear or nonlinear programming method that achieves optimization by going through the middle of the solid defined by the problem rather than around its surface.

Both gradient-based and derivative-free methods have been considered for this problem, and both are applicable in different situations. A gradient-based optimization method, in which the gradient is computed using an adjoint formulation, is often the method of choice since in contrast to numerical perturbation techniques that require as many objective function evaluations as the number of control parameters, the gradient using adjoint-based techniques is obtained only at a small fraction of the time spent for the evaluation of the objective function. The development of adjoint procedures for general compositional flow problems is much more challenging than black-oil simulation because of the need to perform phase-equilibrium (flash) calculations for all grid blocks at every iteration of every time step. Adjoint formulations are challenging to code because they require analytical derivatives of many variables, and the increased complexity of compositional simulators renders these derivatives much more cumbersome to calculate than in the case of a black-oil simulator. Furthermore, the production optimization problem is usually subject to industrial constraints, for example, maximum gas rate specification in injection or production wells, when the control variables are well bottom-hole pressures. At the same time optimising time-varying well settings, such as injection rates, production rates or bottom-hole pressures, is an important aspect of optimal reservoir management that increases significantly the dimension of the search space. It is well known that for non-convex optimisation problems, gradient-based techniques are likely to get trapped in poor local optima. A common practise is to launch several independent optimisations from different initial guesses or to combine ideas from gradient-free algorithms with gradient-based to benefit from the merits of both. An adequate sampling of the search space would require an intractable number of simulations and it is thus impossi-

ble.

### 2.3 Oil-gas compositional simulation equations

The mass conservation equation for component  $i$ , which can exist in any phase  $j$  (here  $j = o, g$ , where  $o$  indicates oil and  $g$  gas), is given by Cao [2002]; Voskov and Tchelepi [2012]; Voskov et al. [2009]:

$$\frac{\partial}{\partial t} \left( \phi \sum_j x_{ij} \rho_j S_j \right) - \nabla \cdot \left( \sum_j x_{ij} \rho_j \mathbf{K} \frac{k_{rj}}{\mu_j} \nabla \Phi_j \right) + \sum_w \sum_j x_{ij} \rho_j q_j^w = 0, \quad i = 1, \dots, n_c. \quad (2.1)$$

In the first (accumulation) term,  $t$  is time,  $\phi$  is porosity,  $x_{ij}$  designates the mole fraction of component  $i$  in phase  $j$ ,  $S_j$  is saturation, and  $\rho_j$  is molar density. In the second (flow) term,  $\mathbf{K}$  is the permeability tensor,  $k_{rj}$  is the relative permeability to phase  $j$ ,  $\mu_j$  the phase viscosity, and the phase potential  $\Phi_j$  is given by  $\Phi_j = p_j - \rho_j g (D - D^0)$ , where  $p_j$  is phase pressure,  $D$  is depth,  $D^0$  is a reference depth, and  $g$  is gravitational acceleration. In the third (source/sink) term,  $q_j^w$  indicates the phase flow rate for well  $w$ . Equation (2.1) is written for each of the  $n_c$  components present in the system.

For a mixture of  $n_c$  components in two fluid phases (oil and gas), thermodynamic equilibrium can be expressed as:

$$f_{io}(p_o, x_{io}) - f_{ig}(p_g, x_{ig}) = 0, \quad (2.2)$$

where  $f_{io}(p_o, x_{io})$  is the fugacity of component  $i$  in the oil phase and  $f_{ig}(p_g, x_{ig})$  is the fugacity of component  $i$  in the gas phase (temperature does not appear because the system is assumed to be isothermal). We additionally must satisfy the saturation constraint ( $S_o + S_g = 1$ ) and the component mole fraction constraints:

$$\sum_{i=1}^{n_c} x_{io} - 1 = 0, \quad \sum_{i=1}^{n_c} x_{ig} - 1 = 0. \quad (2.3)$$

A capillary pressure relationship also appears in cases with nonzero capillary pressure, though here we neglect capillary pressure so  $p_o = p_g$ .

As discussed by many authors (see, e.g., Cao [2002]; Coats [1980]; Voskov and Tchelepi [2012]; Young and Stephenson [1983]), the system described above contains a total of only  $n_c$  primary equations and primary variables per grid block.

These equations and variables are coupled (from block to block), and in a fully-implicit method are all computed simultaneously at each Newton iteration. The remaining (secondary) variables can be computed locally (block by block), and thus very efficiently, once the primary variables are determined. Various options exist for the choice of primary variables (see Voskov and Tchelepi [2012] for discussion). Here we use the so-called natural variable set, which includes, for each grid block, one pressure unknown,  $n_p - 1$  saturation unknowns (where  $n_p$  is the number of phases; here  $n_p = 2$ ), and  $n_c - n_p$  component mole fraction unknowns.

In our formulation, the governing equations (2.1) are solved fully-implicitly, using a backward-Euler time discretization, two-point flux approximation, and single-point upwinding Aziz and Settari [1979]. These treatments are standard in practical reservoir simulation. For the solution of the set of nonlinear equations, we use Newton's method with the solution at the previous time step as the initial guess. A limit on the change of the grid-block saturation and mole fractions over a Newton iteration is applied Younis et al. [2010]. The Newton iterations terminate when the maximum relative norm of the residual is less than  $10^{-6}$  (tight convergence criteria are required for the adjoint solution, discussed below). For the solution of the linear system at each Newton iteration we use GMRES preconditioned by the constrained pressure residual method, as described in Han et al. [2013]. Iteration is terminated when the Euclidean norm of the initial residual has decreased by five orders of magnitude.

We employ a simple time stepping strategy. The time step size at step  $n + 1$  is a multiple of that at  $n$ , provided nonlinear convergence was achieved at step  $n$ . In this way the time step can increase until it reaches the maximum allowable value. If the nonlinear solver fails to converge within a prescribed number of Newton iterations, we divide the time step by a fixed constant. This process is repeated until the nonlinear system converges.

## 2.4 Adjoint equations for the compositional system

We now present the discrete and continuous adjoint equations. Some numerical and coding issues are also discussed.

### 2.4.1 Automatic differentiation

It is quite common for comprehensive computational platforms, in reservoir simulation and other application areas, to undergo frequent modification and enhance-

ment. This poses a problem for adjoint formulations because, when an existing feature is modified the corresponding adjoint code may also be impacted, and when a new feature is added, the associated adjoint code must (in many cases) be written. The maintenance and development of adjoint code poses challenges because the necessary derivatives are generally complicated. This is particularly the case in compositional simulation where variables couple in many ways, including through the nonlinear equation of state.

Automatic differentiation, or AD, is gaining popularity in the field of scientific computing as a means of facilitating the development and enhancement of large code bases. AD enables, for example, the fast (analytical) determination of Jacobian matrix elements from the code defining the residual vector. The use of AD has allowed the fast construction and assessment of different compositional formulations within the same code Voskov et al. [2009]. In this work, we take advantage of AD to automate the construction of many of the derivatives required for the adjoint formulation.

The AD implementation used in our compositional simulator is the ‘automatic differentiation expression templates library’ (ADETL), developed originally by Younis and Aziz Younis and Aziz [2007]. This library generates efficient computer code for the evaluation of the Jacobian matrix and the corresponding partial derivatives from discrete algebraic expressions of the governing conservation equations, associated constraint relations, and equations of state. We refer to Younis and Aziz [2007] for a detailed description of the underlying theory.

### 2.4.2 Discrete adjoint formulation

Following the fully-implicit discretization of the governing equations (using the usual finite volume method, with treatments as noted above), we can express the nonlinear system as:

$$\mathbf{g}_n(\mathbf{x}_n, \mathbf{x}_{n-1}, \mathbf{u}_n) = \mathbf{0}, \quad (2.4)$$

where  $\mathbf{g}_n$  denotes the fully discretized, both in space and time, set of partial differential equations. Here  $\mathbf{x}_n = \mathbf{x}(t_n)$  and  $\mathbf{u}_n = \mathbf{u}(t_n)$  are the states and controls (well settings), respectively, at time step  $n$ . The corresponding time step size is designated  $\Delta t_n$ . We will use throughout the notation  $\partial \mathbf{g}^T / \partial \mathbf{x}$  to denote the matrix  $(\partial \mathbf{g} / \partial \mathbf{x})^T$ .

We are interested in either maximizing or minimizing an objective function  $J$  that is in general a nonlinear function of the states  $\mathbf{x}_n$  and the controls  $\mathbf{u}_n$  of the forward

problem. We assume that  $J$  has the following form:

$$J(\mathbf{x}, \mathbf{u}) = \int_{t_0}^{t_N} f(\mathbf{x}(t), \mathbf{u}(t)) dt + \varphi(\mathbf{x}(t_N)), \quad (2.5)$$

where  $f(\mathbf{x}(t), \mathbf{u}(t))$  is a nonlinear function varying with time and  $\varphi(\mathbf{x}(t_N))$  is a function of only the last state  $\mathbf{x}_N$ . After the solution of the forward problem has been obtained,  $J$  may be approximated by

$$J \approx \sum_{n=1}^N \Delta t_n f_n(\mathbf{x}_n, \mathbf{u}_n) + \varphi(\mathbf{x}_N). \quad (2.6)$$

Using (2.6) we can state the optimal control problem as:

$$\begin{aligned} \text{Extremize } f &= \sum_{n=1}^N \Delta t_n f_n(\mathbf{x}_n, \mathbf{u}_n) + \varphi(\mathbf{x}_N) \\ \text{subject to } \mathbf{g}_n &(\mathbf{x}_n, \mathbf{x}_{n-1}, \mathbf{u}_n) = \mathbf{0}, \\ \text{and } \mathbf{x}_0 &= \mathbf{x}(t_0). \end{aligned} \quad (2.7)$$

In general, a number of linear and nonlinear constraints may need to be included in the optimal control problem. Now, since  $\mathbf{g}_n = \mathbf{0}$ , we can introduce the augmented objective function  $J_A$  by ‘adjoining’ the governing equations to the original objective function  $J$ . The new objective  $J_A$  shares the same extrema as  $J$  and is defined as:

$$J_A = \sum_{n=1}^N \left( \Delta t_n f_n(\mathbf{x}_n, \mathbf{u}_n) + \boldsymbol{\lambda}_n^T \mathbf{g}_n(\mathbf{x}_n, \mathbf{x}_{n-1}, \mathbf{u}_n) \right) + \varphi(\mathbf{x}_N). \quad (2.8)$$

In (2.8), the vectors  $\boldsymbol{\lambda}_n$  are the Lagrange multipliers.

The maximum or minimum of  $J_A$  (and thus  $J$ ) is achieved when the first variation of  $J_A$  is zero ( $\delta J_A = 0$ ). After performing some index-shifting, and grouping terms multiplied by the same variation ( $\delta \mathbf{x}_n, \delta \mathbf{x}_N, \delta \mathbf{u}_n$ ),  $\delta J_A$  can be written as:

$$\begin{aligned} \delta J_A &= \left( \frac{\partial \varphi_N}{\partial \mathbf{x}_N} + \Delta t_N \frac{\partial f_N}{\partial \mathbf{x}_N} + \boldsymbol{\lambda}_N^T \frac{\partial \mathbf{g}_N}{\partial \mathbf{x}_N} \right) \delta \mathbf{x}_N \\ &+ \sum_{n=1}^{N-1} \left( \Delta t_n \frac{\partial f_n}{\partial \mathbf{x}_n} + \boldsymbol{\lambda}_{n+1}^T \frac{\partial \mathbf{g}_{n+1}}{\partial \mathbf{x}_n} + \boldsymbol{\lambda}_n^T \frac{\partial \mathbf{g}_n}{\partial \mathbf{x}_n} \right) \delta \mathbf{x}_n \\ &+ \sum_{n=1}^N \left( \Delta t_n \frac{\partial f_n}{\partial \mathbf{u}_n} + \boldsymbol{\lambda}_n^T \frac{\partial \mathbf{g}_n}{\partial \mathbf{u}_n} \right) \delta \mathbf{u}_n. \end{aligned} \quad (2.9)$$

In order to achieve  $\delta J_A = 0$ , we require  $\delta J_A / \delta \mathbf{x}_n = \mathbf{0}^T$  (for  $n = 1, 2, \dots, N$ ) and  $\delta J_A / \delta \mathbf{u}_n = \mathbf{0}^T$ . To satisfy  $\delta J_A / \delta \mathbf{x}_n = \mathbf{0}^T$  for  $n = 1, 2, \dots, N$ , we require that the Lagrange multipliers satisfy the following equations:

$$\frac{\partial \mathbf{g}_n^T}{\partial \mathbf{x}_n} \boldsymbol{\lambda}_n = - \left( \frac{\partial \mathbf{g}_{n+1}^T}{\partial \mathbf{x}_n} \boldsymbol{\lambda}_{n+1} + \Delta t_n \frac{\partial f_n^T}{\partial \mathbf{x}_n} \right), \quad (2.10)$$

$$\frac{\partial \mathbf{g}_N^T}{\partial \mathbf{x}_N} \boldsymbol{\lambda}_N = - \left( \Delta t_N \frac{\partial f_N^T}{\partial \mathbf{x}_N} + \frac{\partial \varphi_N^T}{\partial \mathbf{x}_N} \right). \quad (2.11)$$

With this choice of the Lagrange multipliers the total variation becomes

$$\delta J_A = \sum_{n=1}^N \left( \Delta t_n \frac{\partial f_n}{\partial \mathbf{u}_n} + \boldsymbol{\lambda}_n^T \frac{\partial \mathbf{g}_n}{\partial \mathbf{u}_n} \right) \delta \mathbf{u}_n,$$

and the gradient of the objective function with respect to the controls is

$$\frac{\delta J_A}{\delta \mathbf{u}} = \left[ \frac{\delta f_1}{\delta \mathbf{u}_1}, \frac{\delta f_2}{\delta \mathbf{u}_2}, \dots, \frac{\delta f_N}{\delta \mathbf{u}_N} \right]. \quad (2.12)$$

The individual entries of  $\delta J_A / \delta \mathbf{u}$  are given by

$$\frac{\delta f_n}{\delta \mathbf{u}_n} = \Delta t_n \frac{\partial f_n}{\partial \mathbf{u}_n} + \boldsymbol{\lambda}_n^T \frac{\partial \mathbf{g}_n}{\partial \mathbf{u}_n}, \quad n = 1, 2, \dots, N. \quad (2.13)$$

By driving  $\delta J_A / \delta \mathbf{u}$  to zero, we achieve the minimum or maximum of  $J_A$  (and thus  $J$ ). In practice,  $\delta J_A / \delta \mathbf{u}$ , along with other quantities related to constraints, are provided to a gradient-based optimization algorithm to determine the next estimate for the controls  $\mathbf{u}$ .

In optimization problems, the well control variables do not typically change at each time step in the flow simulation. Rather, they are defined over longer time periods that are referred to as control steps. Time steps are usually small in order to capture flow dynamics, reduce time-discretization error, and facilitate convergence of the Newton iterations. The gradient at the control period  $m$ ,  $\delta f_n / \delta \mathbf{u}_m$ , is simply the sum of the gradients  $\delta f_n / \delta \mathbf{u}_n$  for all time steps that belong to control period  $m$ .

### 2.4.3 Continuous adjoint formulation

The continuous adjoint formulation employs the continuous representation of the objective function along with the spatially discretized reservoir flow equations.

The optimal control problem can then be stated as:

$$\begin{aligned} & \underset{\mathbf{u}}{\text{minimize}} \quad J(\mathbf{x}, \mathbf{u}) = \int_{t_0}^{t_N} f(\mathbf{x}(t), \mathbf{u}(t)) dt + \varphi(\mathbf{x}(t_N)) \\ & \text{subject to} \quad \mathbf{g}(\dot{\mathbf{x}}(t), \mathbf{x}(t), \mathbf{u}(t)) = \mathbf{0}. \end{aligned}$$

In this case we express the governing set of partial differential equations, for a specified dynamic well-control strategy  $\mathbf{u}(t)$ , as  $\mathbf{g}(\dot{\mathbf{x}}(t), \mathbf{x}(t), \mathbf{u}(t)) = \mathbf{0}$ . We introduce the Lagrange multipliers  $\boldsymbol{\lambda}(t)$  and define the Lagrangian  $L$  as:

$$L(\dot{\mathbf{x}}, \mathbf{x}, \mathbf{u}, \boldsymbol{\lambda}) = f(\mathbf{x}, \mathbf{u}) + \boldsymbol{\lambda}^T \mathbf{g}(\dot{\mathbf{x}}, \mathbf{x}, \mathbf{u}), \quad (2.14)$$

The variables  $\mathbf{u}(t)$ ,  $\mathbf{x}(t)$ ,  $\dot{\mathbf{x}}(t)$  and  $\boldsymbol{\lambda}(t)$  are denoted as  $\mathbf{u}$ ,  $\mathbf{x}$ ,  $\dot{\mathbf{x}}$  and  $\boldsymbol{\lambda}$  to simplify notation. The augmented objective function,  $J_A$ , can be expressed as:

$$J_A(\dot{\mathbf{x}}, \mathbf{x}, \mathbf{u}, \boldsymbol{\lambda}) = \int_{t_0}^{t_N} L(\dot{\mathbf{x}}, \mathbf{x}, \mathbf{u}, \boldsymbol{\lambda}) dt + \varphi(\mathbf{x}_N). \quad (2.15)$$

The first variation of  $J_A$  is given by

$$\begin{aligned} \delta J_A &= \int_{t_0}^{t_N} \left( \frac{\partial L}{\partial \dot{\mathbf{x}}} \delta \dot{\mathbf{x}} + \frac{\partial L}{\partial \mathbf{x}} \delta \mathbf{x} + \frac{\partial L}{\partial \mathbf{u}} \delta \mathbf{u} + \frac{\partial L}{\partial \boldsymbol{\lambda}} \delta \boldsymbol{\lambda} \right) dt \\ &+ \frac{\partial \varphi(\mathbf{x}_N)}{\partial \mathbf{x}_N} \delta \mathbf{x}_N. \end{aligned} \quad (2.16)$$

Note that  $\delta \dot{\mathbf{x}} = d(\delta \mathbf{x})/dt$ , so any variation in the state vector  $\mathbf{x}$  will introduce a variation in its time derivative  $\dot{\mathbf{x}}$ .

After integration by parts, using the fact that the variation of the initial conditions  $\delta \mathbf{x}_0 = \mathbf{0}$ , and taking into account that  $\partial L^T / \partial \boldsymbol{\lambda} = \mathbf{g}(\dot{\mathbf{x}}, \mathbf{x}, \mathbf{u}) = \mathbf{0}$ , the first variation of  $J_A$  can be written as:

$$\begin{aligned} \delta J_A &= \int_{t_0}^{t_N} \left( \frac{\partial L}{\partial \mathbf{x}} - \frac{d}{dt} \frac{\partial L}{\partial \dot{\mathbf{x}}} \right) \delta \mathbf{x} dt \\ &+ \left( \frac{\partial L(\mathbf{x}_N)}{\partial \dot{\mathbf{x}}_N} + \frac{\partial \varphi(\mathbf{x}_N)}{\partial \mathbf{x}_N} \right) \delta \mathbf{x}_N \\ &+ \int_{t_0}^{t_N} \frac{\partial L}{\partial \mathbf{u}} \delta \mathbf{u} dt. \end{aligned} \quad (2.17)$$

To achieve  $\delta J_A / \delta \mathbf{x} = \mathbf{0}$ ,  $\boldsymbol{\lambda}$  must be chosen to satisfy the following:

$$\frac{d}{dt} \left( \frac{\partial \mathbf{g}^T}{\partial \dot{\mathbf{x}}} \boldsymbol{\lambda} \right) - \frac{\partial \mathbf{g}^T}{\partial \mathbf{x}} \boldsymbol{\lambda} - \frac{\partial f^T}{\partial \mathbf{x}} = \mathbf{0} \quad (2.18)$$

$$\frac{\partial \mathbf{g}_N^T}{\partial \dot{\mathbf{x}}_N} \boldsymbol{\lambda}_N = - \frac{\partial \varphi^T(\mathbf{x}_N)}{\partial \mathbf{x}_N}. \quad (2.19)$$

The ordinary differential equation in (2.18) is integrated backwards in time starting from the final time condition (2.19). With the resulting  $\boldsymbol{\lambda}$ , the first variation of the objective function becomes:

$$\delta J_A = \int_{t_0}^{t_N} \left( \frac{\partial f}{\partial \mathbf{u}} + \boldsymbol{\lambda}^T \frac{\partial \mathbf{g}}{\partial \mathbf{u}} \right) \delta \mathbf{u} dt. \quad (2.20)$$

In order to allow a direct comparison of the discrete and continuous adjoint formulations, we integrate the continuous adjoint backwards in time fully implicitly, using the same scheme as is applied for the forward problem. The discrete form of (2.18) is:

$$\frac{\partial \mathbf{g}_n^T}{\partial \mathbf{x}_n} \boldsymbol{\lambda}_n = - \frac{\partial \mathbf{g}_{n+1}^T}{\partial \mathbf{x}_n} \boldsymbol{\lambda}_{n+1} - \Delta t_n \frac{\partial f_n^T}{\partial \mathbf{x}_n}. \quad (2.21)$$

This equation is solved backwards in time, starting from the boundary condition (2.19). Once the Lagrange multipliers have been obtained, the gradient is computed using equations (2.12) and (2.13).

#### 2.4.4 Continuous versus discrete adjoint formulation

The gradients obtained by the discrete adjoint formulation are, as would be expected, fully consistent with the discrete forward problem. Indeed, if we compute the gradients using numerical perturbation of the controls, we find that they coincide with those from the discrete adjoint solution in the first 5-8 significant digits (to achieve this level of agreement, tight tolerances must be used for linear and nonlinear convergence of the forward simulation). There are differences, however, between these gradients and those provided by the continuous adjoint formulation.

To illustrate this, consider the simplified case where  $\varphi(\mathbf{x}_N) = 0$ . The solution of (2.19) in this case will give  $\boldsymbol{\lambda}_N = \mathbf{0}$ , and as a result, the first term in (2.9) will not vanish. There will be a nonzero term left multiplying the variation of  $\delta \mathbf{x}_N$ :

$$\delta J_A = \Delta t_N \frac{\partial f_N}{\partial \mathbf{x}_N} \delta \mathbf{x}_N + \sum_{n=1}^N \left( \Delta t_n \frac{\partial f_n}{\partial \mathbf{u}_n} + \boldsymbol{\lambda}_n^T \frac{\partial \mathbf{g}_n}{\partial \mathbf{u}_n} \right) \delta \mathbf{u}_n. \quad (2.22)$$

It is evident that, as the time step size  $\Delta t_N \rightarrow 0$ , the term multiplying  $\delta \mathbf{x}_N$  will vanish, and the gradient provided by the continuous formulation will become consistent with that from the discrete problem. However, as long as  $\Delta t_N$  is significant, the two gradients will not coincide, especially at the last time step.

We implemented both the continuous and discrete adjoint formulations into our optimization framework. Using a small  $\Delta t_N$ , we observed that the computed gradients were very similar, consistent with (2.22). Even using small  $\Delta t_N$ , however, we did not observe any advantage of the continuous formulation over the discrete formulation. In cases where  $\Delta t_N$  was not small, the continuous formulation required more iterations of the optimizer, presumably because of errors in  $\delta J_A / \delta \mathbf{u}$ . In light of these observations, we do not present any detailed results using the continuous adjoint formulation since we do not see any advantages to this approach for our problem. We note that these findings are consistent with those reported in Hager [2000] and Walther [2007] for general Runge-Kutta time stepping methods, in Nadarajah and Jameson [2000], where the discrete and continuous adjoint approaches were applied to automatic aerodynamic optimization, and in Petra and Stadler [2011] for general variational inverse problems governed by partial differential equations. A similar gradient discrepancy between discretization/optimization versus optimization/discretization can also occur with respect to the spatial discretization – see the discussion for a shape optimization problem in Gunzburger [2003].

#### 2.4.5 Solution of adjoint equations

The solution of the linear system of equations that arises when solving (2.10) constitutes the largest computational demand in the adjoint problem. The matrix appearing in this equation at time step  $n$ ,  $\partial \mathbf{g}_n^T / \partial \mathbf{x}_n$ , is the transpose of the Jacobian matrix for the converged forward problem,  $\partial \mathbf{g}_n / \partial \mathbf{x}_n$ . In our implementation, the converged states are written to disk during the solution of the forward problem. These converged states are then read back, during the solution of the adjoint problem, and  $\partial \mathbf{g}_n / \partial \mathbf{x}_n$  is reconstructed, along with all other derivatives appearing in equations (2.10), (2.11) and (2.13). This enables the evaluation of the Lagrange multipliers  $\boldsymbol{\lambda}_n$  and the gradients  $\partial f_n / \partial \mathbf{u}_n$ .

For the solution of the linear system in (2.10), we use GMRES preconditioned by the transpose of the CPR (constrained pressure residual) preconditioner, as described in Han et al. [2013]. In these linear solutions, we require very high accuracy to guarantee that residual errors accumulated over hundreds of time steps do not pollute the gradients (which would influence the computed optimum). For this reason, we continue iterating the linear solver until the Euclidean norm of the initial residual has decreased by 10 orders of magnitude. This is significantly higher accuracy than is required for the forward problem.

## 2.5 Gradient-based optimization and related software

The SNOPT optimizer is used in this work for solving the nonlinear constrained optimization problem, and in this section we will provide a concise overview of the underlying theory. This discussion loosely follows Gill et al. [2005], which provides a much more in-depth description. SNOPT uses a sparse sequential quadratic programming (SQP) algorithm that exploits sparsity in the constraint Jacobian and maintains a limited-memory quasi-Newton approximation to the Hessian of the Lagrangian. The QP subproblems are solved using an inertia-controlling reduced-Hessian active-set method (SQOPT) that allows for variables appearing linearly in the objective and constraint functions.

We now discuss the main features of the SQP method used to solve our nonlinear program (NP). This discussion follows Gill et al. [2005]. All realistic recovery optimization problems involve bound constraints on the inputs, and often several other linear or nonlinear equality or inequality constraints, which together constitute a so-called general nonlinear program (GNP). Here we take the problem to be

$$\begin{array}{ll} \text{(NP)} & \underset{\mathbf{u}}{\text{minimize}} \quad f(\mathbf{u}) \\ & \text{subject to} \quad \mathbf{c}(\mathbf{u}) \geq \mathbf{0}, \end{array}$$

where  $\mathbf{u} \in \mathbb{R}^n$ ,  $\mathbf{c} \in \mathbb{R}^m$ , while the objective function  $f(\mathbf{u})$  and the constraints  $c_i(\mathbf{u})$ ,  $i = 1, 2, \dots, m$  have continuous second derivatives. The gradient of  $f$  is denoted by the vector  $\nabla f(\mathbf{u})$ , and the gradients of each element of  $\mathbf{c}$  form the rows of the Jacobian matrix  $\mathbf{J}(\mathbf{u})$ .

An SQP method obtains search directions (for the primal  $\mathbf{u}$  and dual variables  $\boldsymbol{\pi}$ ) from an iterative sequence of QP subproblems. Each QP subproblem, in turn, iteratively minimizes a convex quadratic model of a certain Lagrangian function subject to linearized constraints associated with (NP), namely,

$$\mathcal{L}(\mathbf{u}, \mathbf{u}_k, \boldsymbol{\pi}_k) = f(\mathbf{u}) - \boldsymbol{\pi}_k^T \mathbf{d}_L(\mathbf{u}, \mathbf{u}_k), \quad (2.23)$$

defined in terms of the constraint linearization  $\mathbf{c}_L(\mathbf{u}, \mathbf{u}_k)$  and the departure from linearity  $\mathbf{d}_L(\mathbf{u}, \mathbf{u}_k)$ :

$$\begin{aligned} \mathbf{c}_L(\mathbf{u}, \mathbf{u}_k) &= \mathbf{c}_k + \mathbf{J}_k(\mathbf{u} - \mathbf{u}_k), \\ \mathbf{d}_L(\mathbf{u}, \mathbf{u}_k) &= \mathbf{c}(\mathbf{u}) - \mathbf{c}_L(\mathbf{u}, \mathbf{u}_k), \end{aligned}$$

subject to linearized constraints. In this formulation  $k$  is the SQP (major) iteration counter, and  $\boldsymbol{\pi}$  are Lagrangian multipliers to adjoin  $\mathbf{d}_L$  to  $f$ . The first and second

derivatives of the modified Lagrangian with respect to  $\mathbf{u}$  are

$$\begin{aligned}\nabla \mathcal{L}(\mathbf{u}, \mathbf{u}_k, \boldsymbol{\pi}_k) &= \nabla f(\mathbf{u}) - (\mathbf{J}(\mathbf{u}) - \mathbf{J}_k)^T \boldsymbol{\pi}_k, \\ \nabla^2 \mathcal{L}(\mathbf{u}, \mathbf{u}_k, \boldsymbol{\pi}_k) &= \nabla^2 f(\mathbf{u}) - \sum_i (\boldsymbol{\pi}_k)_i \nabla^2 c_i(\mathbf{u}).\end{aligned}$$

Observe that  $\nabla^2 \mathcal{L}$  is independent of  $\mathbf{u}_k$  and is the same as the Hessian of the conventional Lagrangian. At  $\mathbf{u} = \mathbf{u}_k$ , i.e., after convergence of the inner iterations, the modified Lagrangian has the same function and gradient values as the objective:  $\mathcal{L}(\mathbf{u}_k, \mathbf{u}_k, \boldsymbol{\pi}_k) = f_k$ ,  $\nabla \mathcal{L}(\mathbf{u}_k, \mathbf{u}_k, \boldsymbol{\pi}_k) = \nabla f_k$ . The modified augmented Lagrangian is ‘less’ nonlinear than the augmented Lagrangian itself because linear terms in the constraints disappear, especially in the quadratic penalty term. The number of nonlinear variables in the modified augmented Lagrangian is the same as in the original problem.

The merit function

$$\mathcal{M}_\rho(\mathbf{u}, \boldsymbol{\pi}, \mathbf{s}) = f(\mathbf{u}) - \boldsymbol{\pi}^T (\mathbf{c}(\mathbf{u}) - \mathbf{s}) + \frac{1}{2} \sum_{i=1}^m \rho_i (c_i(\mathbf{u}) - s_i)^2, \quad (2.24)$$

where  $\boldsymbol{\rho}$  and  $\mathbf{s}$  are vectors of penalty parameters and slack variables, respectively, is reduced along each search direction to ensure convergence from any starting point.

In summary, the basic structure of an SQP method involves major and minor iterations. The major iterations generate a sequence of iterates  $(\mathbf{u}_k, \boldsymbol{\pi}_k)$  that converge to the optimal solution  $(\mathbf{u}^*, \boldsymbol{\pi}^*)$ . At each major iterate a QP subproblem is solved to generate a search direction towards the next iterate  $(\mathbf{u}_{k+1}, \boldsymbol{\pi}_{k+1})$ . Solving such a subproblem is itself an iterative procedure, and the minor iterations of an SQP method are the iterations of the QP method. SNOPT requires first-order derivatives of the nonlinear objective and constraint functions with respect to the control variables, which are provided by our adjoint procedure.



# Chapter 3

## Benchmark Problems

We implement an adjoint treatment for multicomponent oil-gas compositional systems through use of a recently developed automatic differentiation capability [Younis et al., 2010]. The application of automatic differentiation in the context of Stanford’s General Purpose Research Simulator (AD-GPRS) [Cao, 2002], a modular simulator with many advanced features, enables us to construct a gradient-based optimization framework suitable for use in compositional problems. In a discrete implementation, the governing equations for the so-called adjoint system are constructed based on the discretized-in-time forward model equations. In all examples we maximize cumulative oil recovery under CO<sub>2</sub> injection.

The oil industry considers as optimum production implementation the so called “full blast method” where the injectors operate at the upper bound of the acceptable pressure while the producers operate at the lower pressure boundary. The concept of “full blast” is based on pressure maintenance. The primary objective of this thesis is to present the advantages of optimization over the “full blast” method. We will present results for two benchmarks of increased complexity.

Initially, the objective function of Cumulative oil is optimized with the use of AD-GPRS. The Net Present Value function is a nonlinear function of the states  $\mathbf{x}_n$  and the controls  $\mathbf{u}_n$  of the forward problem and has the following format:

$$f_n = F(x_n, x_{n+1}, u_u), \quad (3.1)$$

$$f_n = \frac{dt_n}{(1 + \alpha)^{t_n}} \left[ \sum_{(j=1)}^{N_p} P^T Q_{p,j}^n + \sum_{(j=1)}^{N_i} C^T Q_{i,j}^n \right], \quad (3.2)$$

where  $N_p$  is the number of producers,  $N_i$  is the number of injectors,  $P$  the production prices for each phase [\$/ barrel],  $C$  is the injection prices for each phase [\$/ barrel],  $Q_{p,j}$  and  $Q_{i,j}$  are the production and injection rates of each phase at surface conditions, where  $j$  stands for the  $j_{th}$  injector/producer,  $\alpha$  is the discount factor,  $dt_n$  is the  $n_{th}$  timestep and  $t_n$  is the simulation time at after the  $n_{th}$  timestep.

The gradient-based optimization will find only a local optimum thus, we run each case nine times, using a different initial guess for the well controls. Each initial guess corresponds to a combination of BHPs from the set  $\{p_I^u, p_I^l, p_I^a\}$  for the injectors and from the set  $\{p_P^u, p_P^l, p_P^a\}$  for the producers, where  $p^u$ ,  $p^l$  and  $p^a$  designate the upper and lower limits on the initial BHPs, and the average between these limits, respectively. We set  $p^l = p_{init} + 1$  bar for the injectors and  $p^u = p_{init} - 1$  bar for the producers, where  $p_{init}$  is the initial reservoir pressure as listed in Table 3.1. Note that these ‘limits’ are simply used to prescribe initial guesses for the optimization – they are not related to the actual BHP bound constraints.

Run	Initial guess
1	$[p_I^l, p_P^l]$
2	$[p_I^l, p_P^a]$
3	$[p_I^l, p_P^u]$
4	$[p_I^a, p_P^l]$
5	$[p_I^a, p_P^a]$
6	$[p_I^a, p_P^u]$
7	$[p_I^u, p_P^l]$
8	$[p_I^u, p_P^a]$
9	$[p_I^u, p_P^u]$

Table 3.1: Initial guesses for the optimizations for all cases considered.

Subsequently, we optimize the objective of Cumulative oil by implementing a “geology continuation” method. In this novel method the geology alters gradually, from the homogeneous version of the benchmark to its final geology. The optimum controls from each optimized sub-geology are sequentially introduced as initial controls to the next sub-geology. This optimization approach was inspired by similar methods implemented in continuum mechanics and was based on the fact that in an homogeneous benchmark, it is more probable for the optimization process to end up in a global optimum. Thus, by changing gradually the geology, the outcome will remain in the vicinity of the global optimum.

### 3.1 Example 1 - $\Pi$ obstacle

In the first example we maximize cumulative oil recovery under  $\text{CO}_2$  injection. The two-dimensional geological model is depicted in Fig. 3.1. A  $\Pi$ -shaped region is located at the center of a homogeneous reservoir. The model is discretized on a grid of dimensions  $80 \times 80$ . The permeability in most of the domain (red cells) is set to 4000 mD, while the permeability for the blue cells that comprise the  $\Pi$ -shaped region is set to 1 mD. In all of our examples we describe the permeability with a diagonal tensor:  $\mathbf{K} = \text{diag}(\mathbf{k}_x, \mathbf{k}_y, \mathbf{k}_z)$ ; here, in addition, the permeability is isotropic and uniform within both of the regions. Four injection wells are placed at the corners of the model and the single production well is located inside the  $\Pi$ -shaped region. The model includes a total of four components (three hydrocarbon components plus  $\text{CO}_2$ ), as specified in Table 3.2. Further details on the reservoir model are provided in Table 3.3.

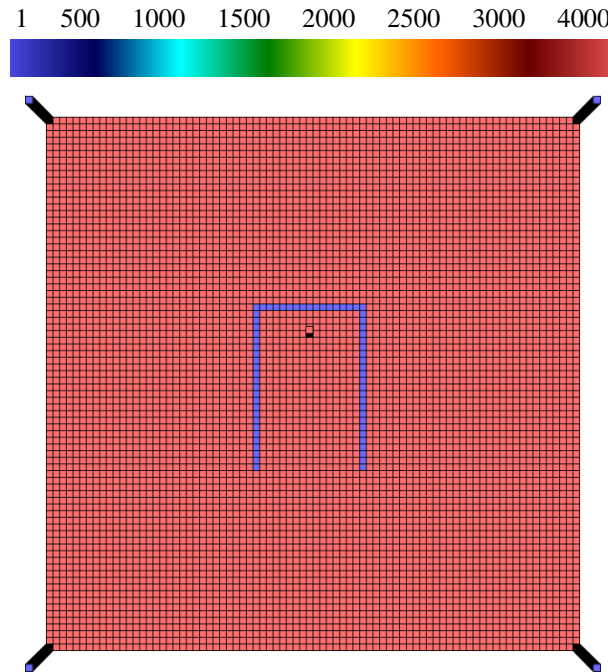


Figure 3.1: Injection wells (blue) and production well (red) for Example 1. Background shows  $\mathbf{k}_x$  ( $\mathbf{k}_x = \mathbf{k}_y$ ).

Component	CO <sub>2</sub>	C <sub>1</sub>	C <sub>4</sub>	C <sub>10</sub>
Initial composition (%)	1	20	29	50
Injection composition (%)	100	-	-	-

Table 3.2: Fluid description for Example 1

Parameter	Value	Units
Grid size	80 × 80 × 1	—
Δx	6	m
Δy	6	m
Δz	4	m
Depth	4000	m
Initial pressure	100	bar
Temperature	100	°C
Rock compressibility	7.2 × 10 <sup>-5</sup>	1 / bar
Simulation time	256	d
Pressure upper bound	120	bar
Pressure lower bound	90	bar
Residual gas saturation	0	—
Residual oil saturation	0	—
End point rel perm gas	1	—
End point rel perm oil	1	—
Corey exponent gas	2	—
Corey exponent oil	2	—
Well locations [grid block no.]	<i>i</i>	<i>j</i>
Injector 1	1	1
Injector 2	1	80
Injector 3	80	1
Injector 4	80	80
Producer 1	40	48

Table 3.3: Model parameters for example 1.

The control parameters in the optimization problem are the well BHPs. These are constrained to lie between an upper bound of 120 bar and a lower bound of 90 bar. The total simulation period is 256 days, and the well controls are determined at initial time and for every subsequent 32-day interval. There are thus a total of eight control steps and 40 control parameters.

### 3.1.1 Optimization of cumulative oil

As a reference we run the simulation with the production wells operating at the minimum BHP and the injection wells at the maximum BHP. The cumulative oil production for this case is given in the first row ('Reference') of Table 3.4. We next perform optimizations that honor the bound constraints for all nine initial guesses. The simulation and the optimization results, are presented in Table 3.4 in the columns labeled 'Reference' and 'One step' respectively. In order to evaluate the time discretization error, the final simulations are repeated for a smaller timestep. The results are presented in Table 3.4, in the columns labeled '*Reference*' and '*Onestep*' respectively. Also a relative error is presented in the last column of Table 3.4.

The optimization procedure resulted the to same controls of full blast method (starting from the initial guess of  $[p_I^u, p_P^l]$ ) and subsequently the exact same result on account to the simplicity of the benchmark. A visual representation of the cumulative oil, the BHPs, the gas rates and the oil rates for the optimal for reference case are shown in Fig. 3.2, Fig. 3.3, Fig. 3.4, Fig. 3.5.

Run	Reference	<i>Reference</i>	One step	<i>Onestep</i>	Error
<i>Reference</i>	<b>11.91</b>				
$[p_I^a, p_P^a]$	10.09	10.12	10.26	10.28	0.3%
$[p_I^a, p_P^l]$	10.84	10.88	10.86	10.88	0.36%
$[p_I^a, p_P^u]$	8.97	8.99	8.93	8.94	0.22%
$[p_I^l, p_P^a]$	6.15	6.15	6.15	6.15	0%
$[p_I^l, p_P^l]$	8.81	8.83	11.46	11.52	0.52%
$[p_I^l, p_P^u]$	2.45	2.45	8.16	8.18	0.24%
$[p_I^u, p_P^a]$	11.6	11.64	11.62	11.64	0.34%
$[p_I^u, p_P^l]$	<b>12.11</b>	<b>11.91</b>	<b>12.11</b>	<b>11.91</b>	1.65%
$[p_I^u, p_P^u]$	11.21	11.24	11.22	11.24	0.27%

Table 3.4: Oil production in  $10^4 \text{ m}^3$  (Example 2) for the objective function of Cumulative oil (Example 1, 256 days) for nine initial guesses, using the ADGPRS. The simulation and optimization for 2 different time steps and their relative time discretization error are presented.

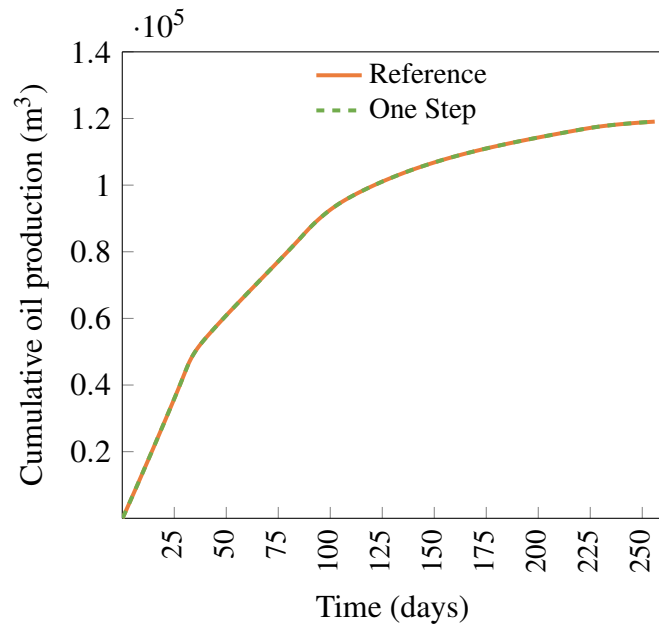


Figure 3.2: Oil production versus time for Example 1. Results are for reference case (orange curve), best optimized solution (green curve).

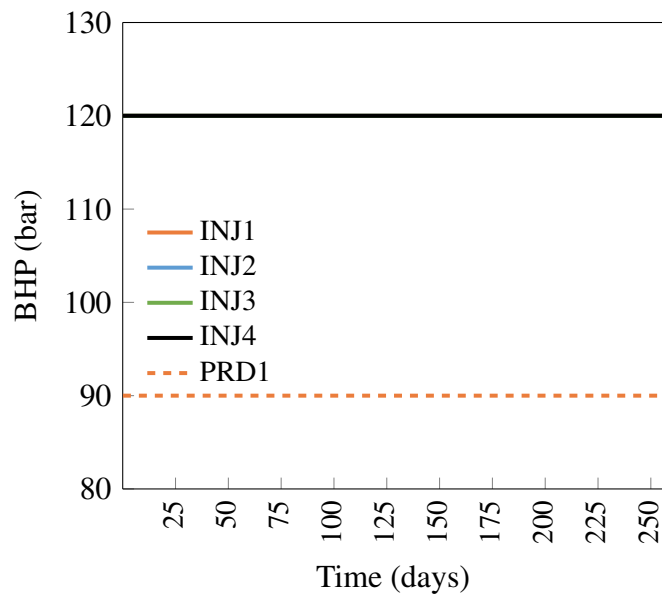


Figure 3.3: BHPs of injectors and producer versus time for the reference case of Example 1.

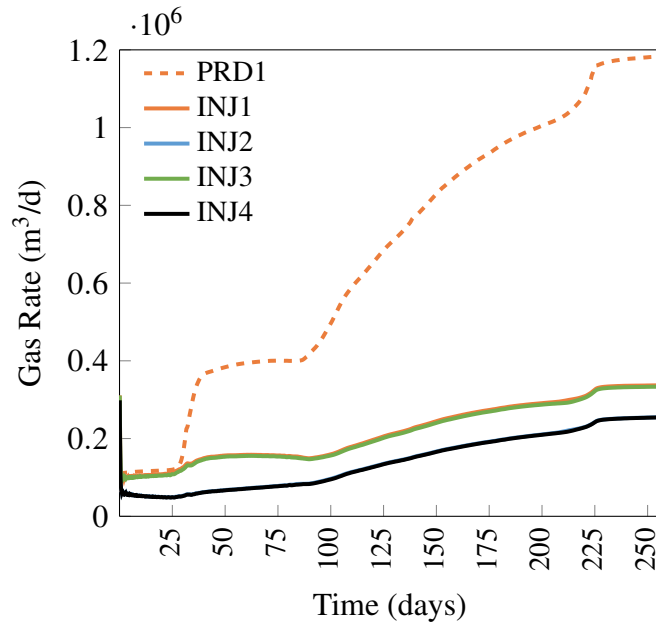


Figure 3.4: Gas rates in m<sup>3</sup>/d of injectors and producer versus time, for the reference case of Example 1.

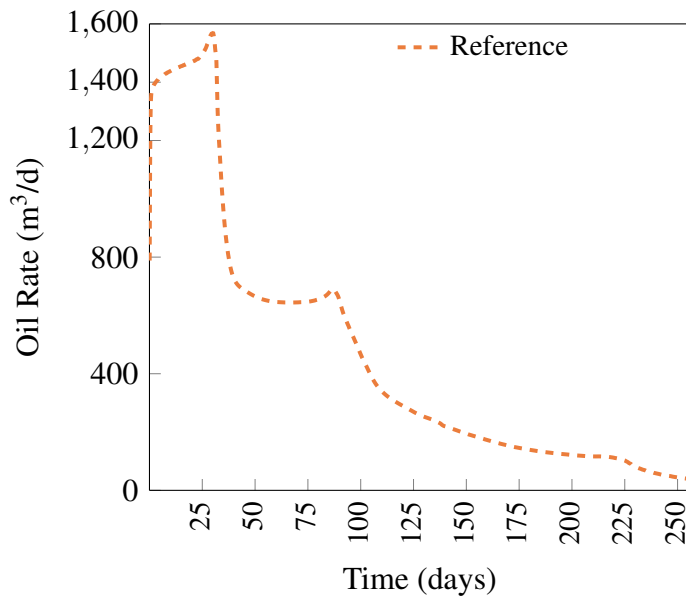


Figure 3.5: Oil rates in m<sup>3</sup>/d of the producer versus time, for the reference case of Example 1.

### 3.1.2 Optimization with geological continuation

In this part of the thesis we examine if the results can be further improved by using a continuation in geology. In this process we use twenty different geologies, starting from the homogeneous version of the benchmark and gradually altering it until we reach the original one. The optimal controls for each sub-geology are introduced as initial guesses for the next sub-geology in sequential process. The concept is that in a homogeneous reservoir, permeability, porosity and well indexes exhibit the same values in all grid blocks, thus, the optimization with gradient based algorithms should result to a global optimum and avoid falling into poor local optima. Specifically, for this example, twenty sequential optimizations have been made and for the first sub-geology (homogeneous) the controls of “full blast” were set as initial conditions. The gradual change of the cumulative oil is presented in Fig. 3.6. For the final geology an extra simulation step with an improved time step is used in order to obtain a more accurate value of the objective. Also a visual representation of the depleted sub-reservoirs is shown at Fig. 3.7 where the gradual change of the oil saturation is depicted.

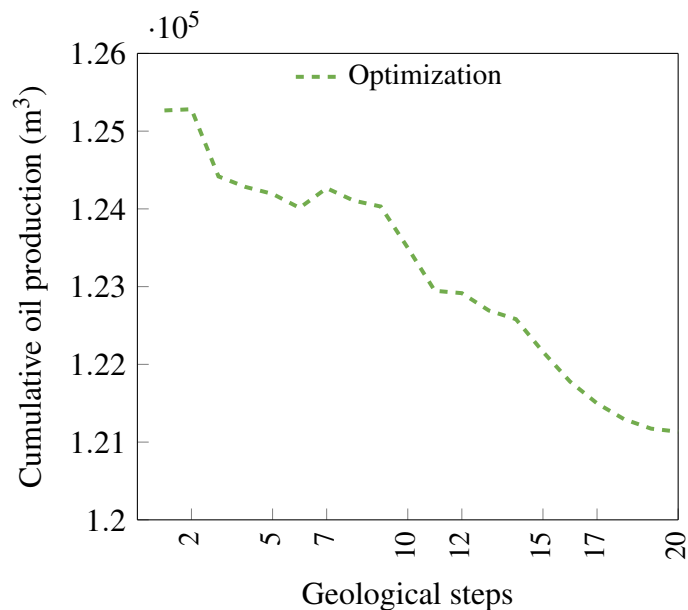
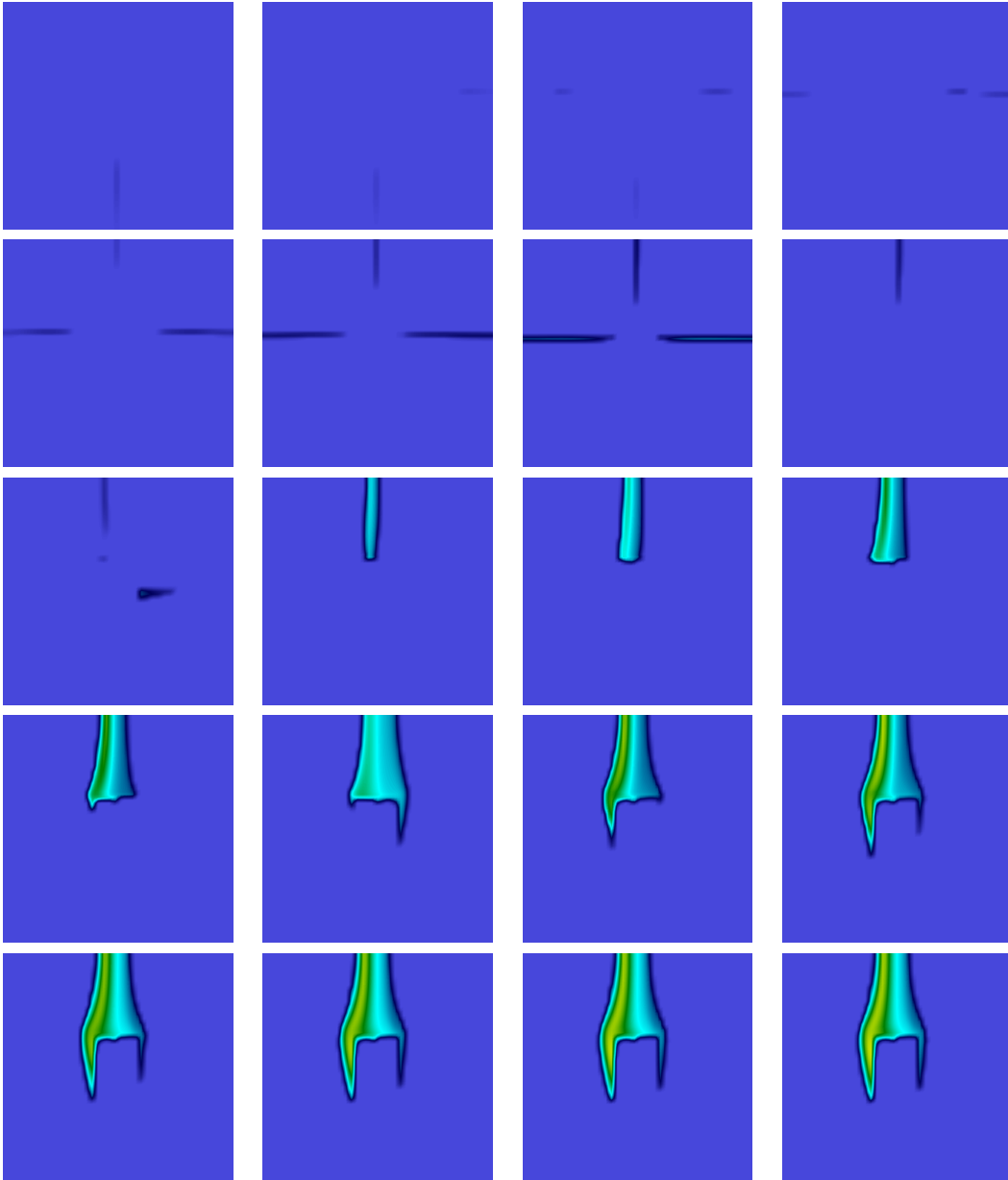


Figure 3.6: Cumulative oil production in  $\text{m}^3$  for each optimized geology step (Example 1, 256 days).

Figure 3.7: Oil saturation maps for 20 optimized geology steps for example 1.



The resulted cumulative oil for each case is given in Table 3.5, where results from the simulation, the optimization and optimization with the geological continuation method, are presented in the respectively labeled columns. The optimization process of geological continuation slightly outweighed the reference method, resulting an improved value of  $12.11 \cdot 10^4 \text{ m}^3$  instead of  $11.9 \cdot 10^4 \text{ m}^3$ . The gradual change of the cumulative oil is presented in Fig. 3.20. A comparative representation of the results is demonstrated in Fig. 3.8. Also, the BHPs, the oil and gas rates for this new approach are presented in Fig. 3.9, 3.10 and in Fig. 3.11.

$[p_I^u, p_P^l]$	Reference	One Step	Continuation
Cumulative oil	<b>11.9</b>	11.91	12.21

Table 3.5: Oil production in  $10^4 \text{ m}^3$  for simulation, optimization without continuation and optimization with twenty geological steps. Reference result shown in bold.

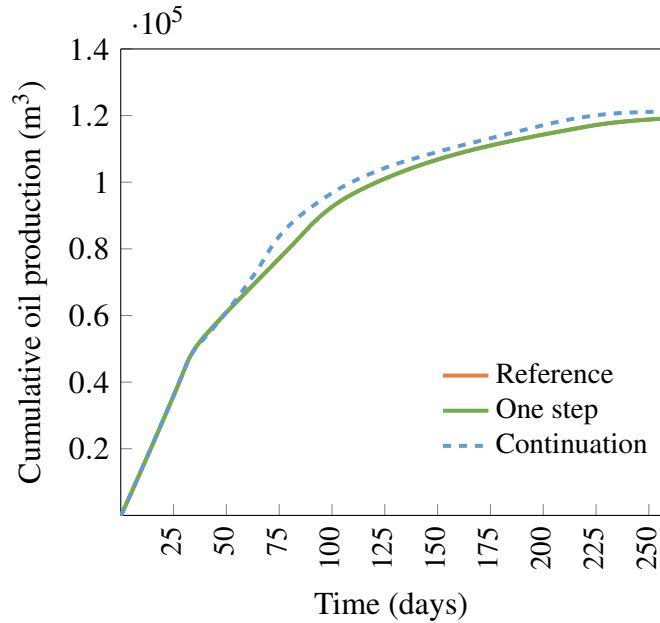


Figure 3.8: Oil production versus time for Example 1. Results are for reference case (orange curve), optimized solution (green curve) and optimized solution with geological continuation (blue dashed curve).

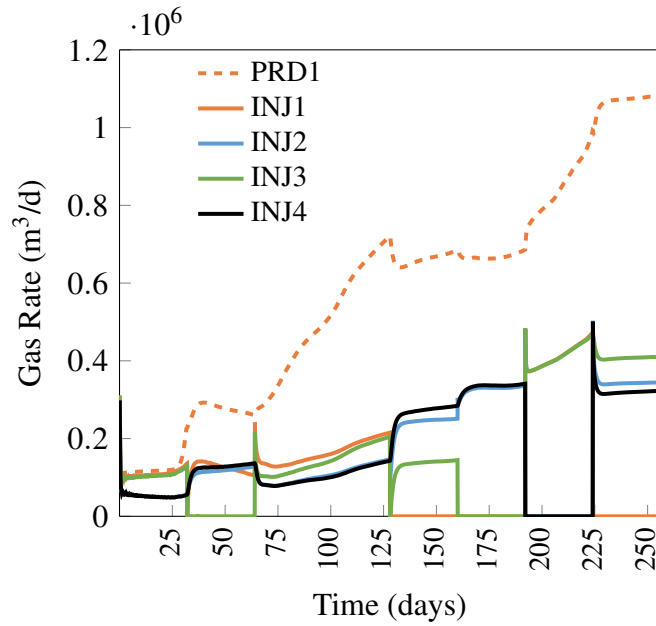


Figure 3.10: Gas rates in  $\text{m}^3/\text{d}$  of the injectors and the producer versus time, for the optimal solution with geological continuation of Example 1.

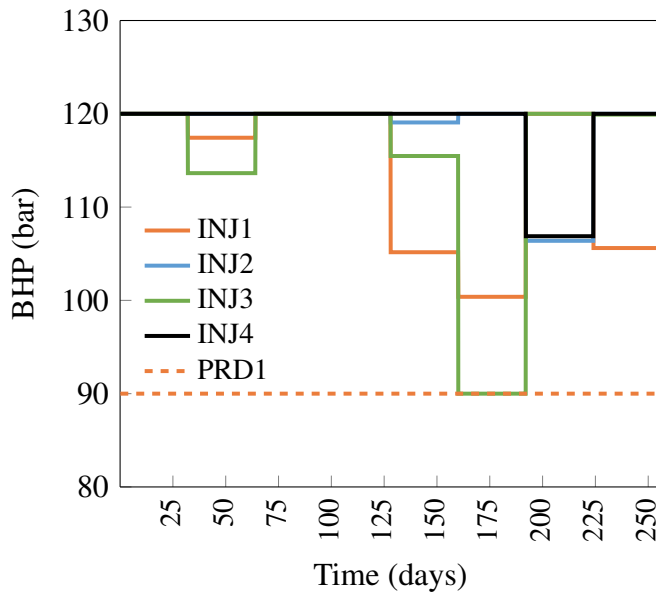


Figure 3.9: BHPs of injectors and producer, versus time, for the optimal solution with geological continuation optimization of Example 1.

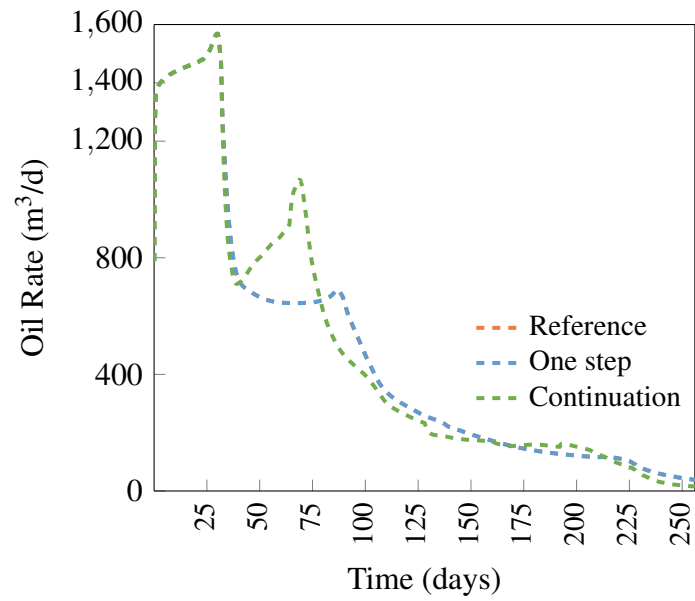


Figure 3.11: Oil rates in  $\text{m}^3/\text{d}$  of the producer versus time, for the reference, the optimized and the geological continuation case of Example 1.

### 3.2 Example 2 - Top layer of SPE 10 model

As we did in the first example, in this example we also maximize cumulative oil recovery under CO<sub>2</sub> injection. The two-dimensional geological model is the top layer of the model defined in the SPE comparative solution project Christie and Blunt [2001], referred to as SPE 10. The model includes a total of four components, as specified in Table 3.6.

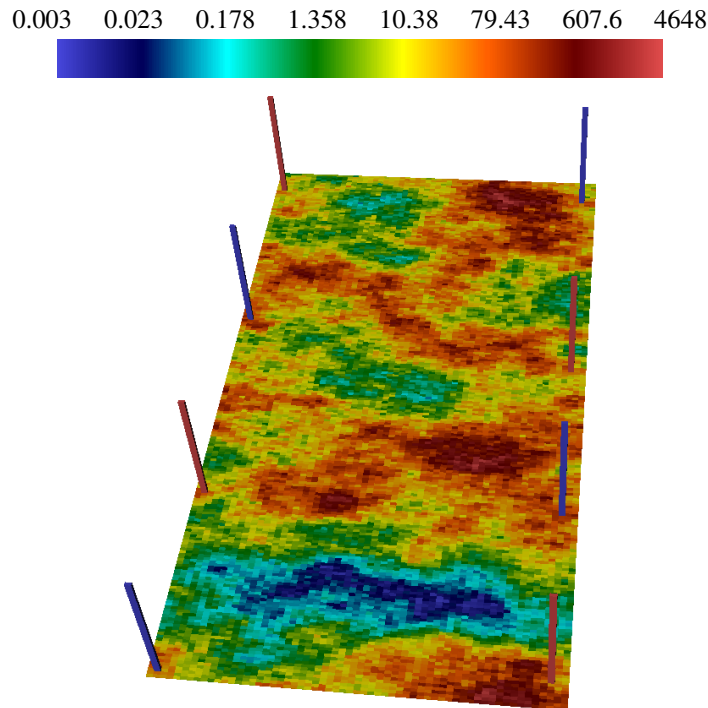


Figure 3.12: Injection wells (blue) and production wells (red) for Example 2. Background shows  $\log \mathbf{k}_x$  ( $\mathbf{k}_x = \mathbf{k}_y$ ).

Component	CO <sub>2</sub>	C <sub>1</sub>	C <sub>4</sub>	C <sub>10</sub>
Initial composition (%)	1	20	29	50
Injection composition (%)	99	1	-	-

Table 3.6: Fluid description for Example 2.

Details of the reservoir model are provided in Table 3.7. The well locations, along with a map of the permeability field, are depicted in Fig. 3.12. The control parameters in this optimization problem are the well BHPs, constrained to lie between

50 bar and 150 bar. The total simulation period is 1000 days. The well controls are determined at initial time and then at every 100-day interval. Subsequently, there is a total of ten control steps and 80 control parameters in this example.

Parameter	Value	Units
Grid size	$60 \times 220 \times 1$	—
$\Delta x$	6.096	m
$\Delta y$	3.048	m
$\Delta z$	0.6096	m
Depth	2574	m
Initial pressure	100	bar
Temperature	100	°C
Rock compressibility	$7.2 \times 10^{-5}$	1 / bar
Simulation time	1000	d
Pressure upper bound	150	bar
Pressure lower bound	50	bar
Residual gas saturation	0	—
Residual oil saturation	0	—
End point rel perm gas	1	—
End point rel perm oil	1	—
Corey exponent gas	2	—
Corey exponent oil	2	—
Well locations [grid block no.]	<i>i</i>	<i>j</i>
Injector 1	58	9
Injector 2	58	126
Injector 3	2	67
Injector 4	2	211
Producer 1	2	3
Producer 2	58	67
Producer 3	2	143
Producer 4	58	210

Table 3.7: Model parameters for Example 2.

### 3.2.1 Optimization of cumulative oil

We first generate the reference solution as in the previous example. The cumulative oil production for this case is given in the first row ('Reference') of Table 3.8. We next perform optimizations for the previously mentioned nine initial guesses that honor the bound constraints for BHPs. The cumulative oil production for both the simulation and the optimization, for all nine initial guesses, are presented in Table 3.8, in the respectively labeled columns. Similarly to the previous example, in order to evaluate the time discretization error, the simulations for the optimal controls of each case were repeated for a smaller timestep. The results are presented in Table 3.8, in the columns labeled '*Reference\**' and '*Onestep\**' respectively. The optimization process resulted an improved cumulative oil production of  $51.1910^4 \text{ m}^3$  ( $[p_I^u, p_P^l]$ ). A visual representation of the cumulative oil for the optimum solution and the reference is depicted in Fig. 3.13. Additionally, the BHPs, the oil and gas rates for both cases are presented in Fig. 3.14, 3.15, 3.16, 3.17, 3.18, 3.19.

Run	Reference	<i>Reference*</i>	One step	<i>Onestep*</i>
Reference	<b>50.86</b>			
$[p_I^a, p_P^a]$	38.87	38.83	51.18	51.17
$[p_I^a, p_P^l]$	45.79	45.77	51.19	51.18
$[p_I^a, p_P^u]$	29.2	29.17	51.19	51.18
$[p_I^l, p_P^a]$	28.84	28.85	51.01	50.99
$[p_I^l, p_P^l]$	38.31	38.32	51.18	51.17
$[p_I^l, p_P^u]$	28.25	28.3	50.91	50.88
$[p_I^u, p_P^a]$	46.29	46.19	51.19	51.18
$[p_I^u, p_P^l]$	50.91	<b>50.86</b>	51.2	<b>51.19</b>
$[p_I^u, p_P^u]$	39.68	39.57	51.19	51.18

Table 3.8: Cumulative oil production in  $10^4 \text{ m}^3$  for nine initial guesses (Example 2). Results for simulation and optimization. Reference and optimal results are shown in bold.

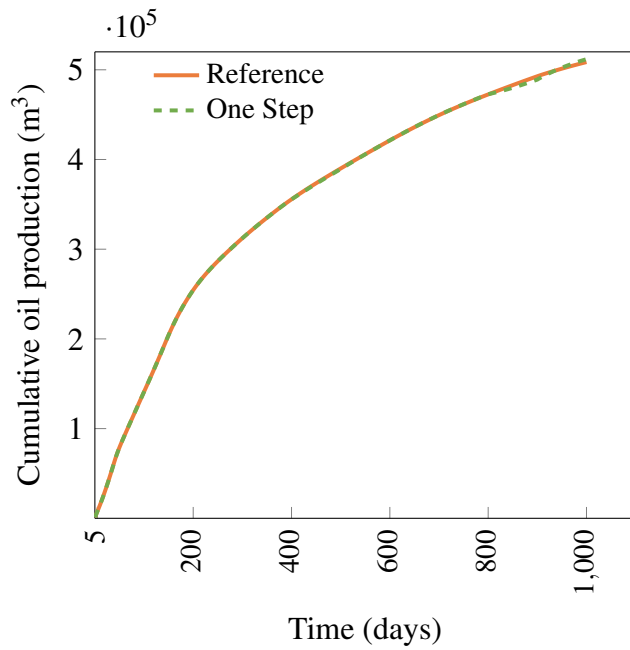


Figure 3.13: Oil production versus time for Example 2. Results are for reference case (orange curve) and best optimized solution (green curve)

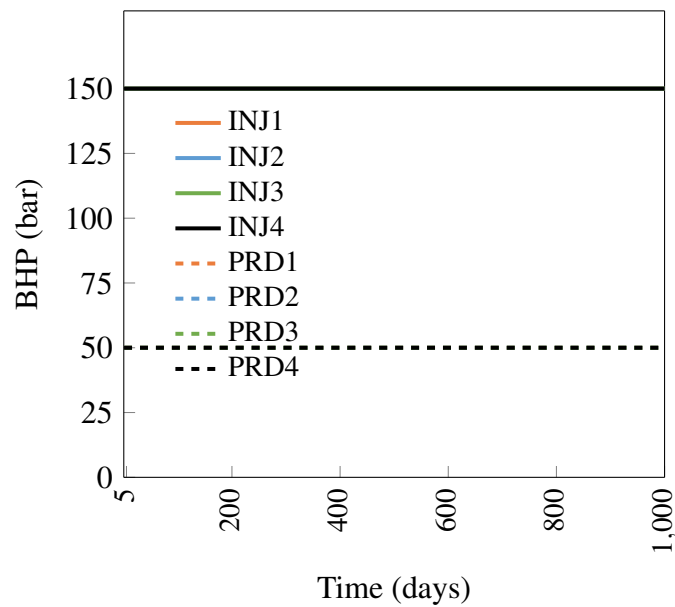


Figure 3.14: BHPs of injectors and producers, versus time, for the reference case of Example 2.

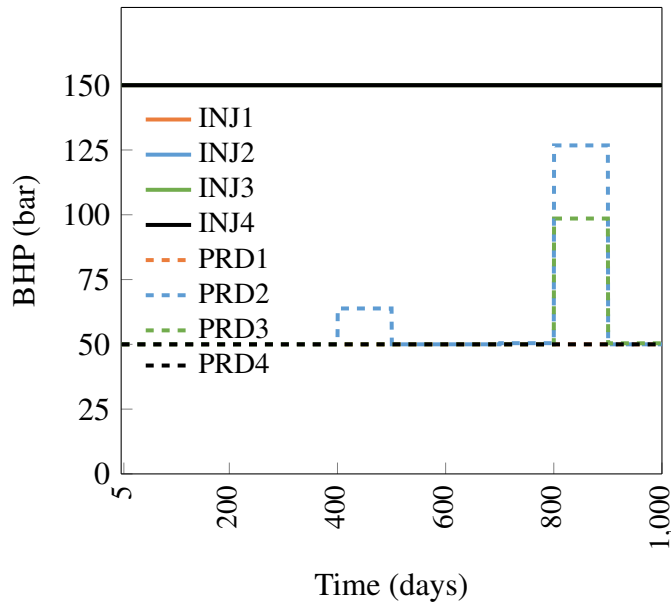


Figure 3.15: BHPs of injectors and producers, versus time, for the optimal solution of Example 2.

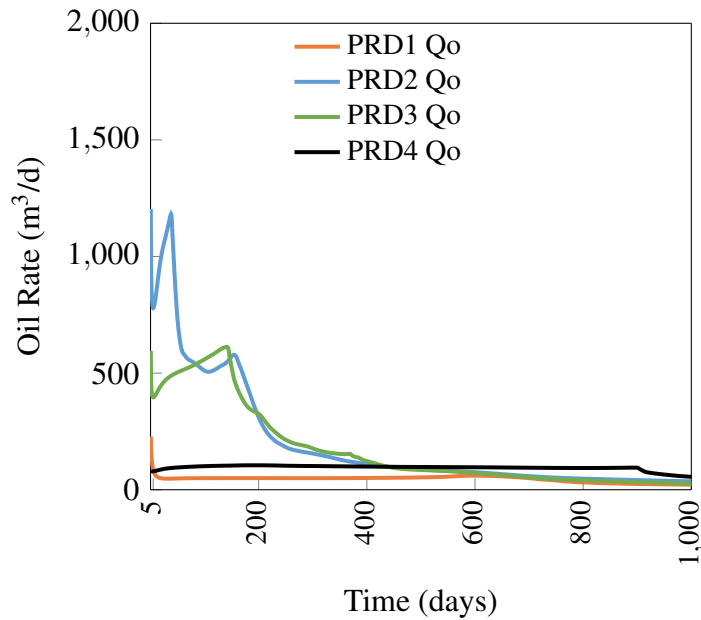


Figure 3.16: Oil rates in m<sup>3</sup>/d for the producers versus time for the reference case of Example 2.

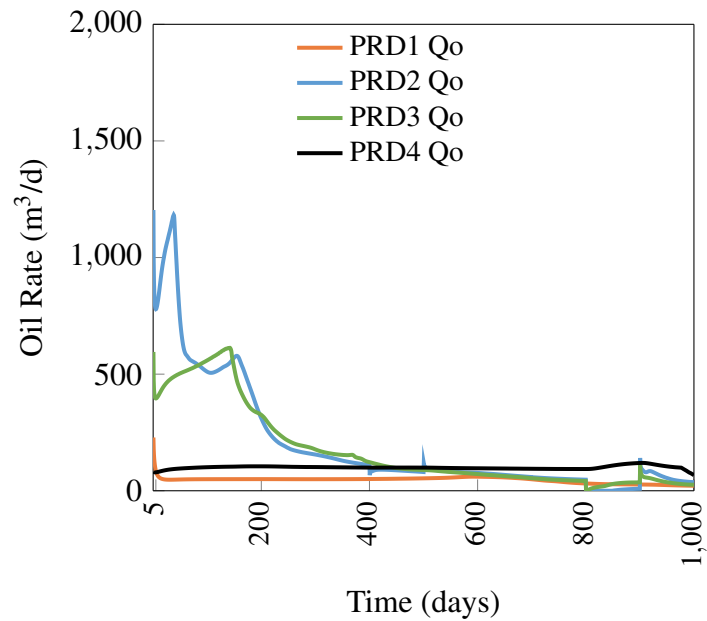


Figure 3.17: Oil Rates in  $\text{m}^3/\text{d}$  for the producers versus time for the optimal case of Example 2.

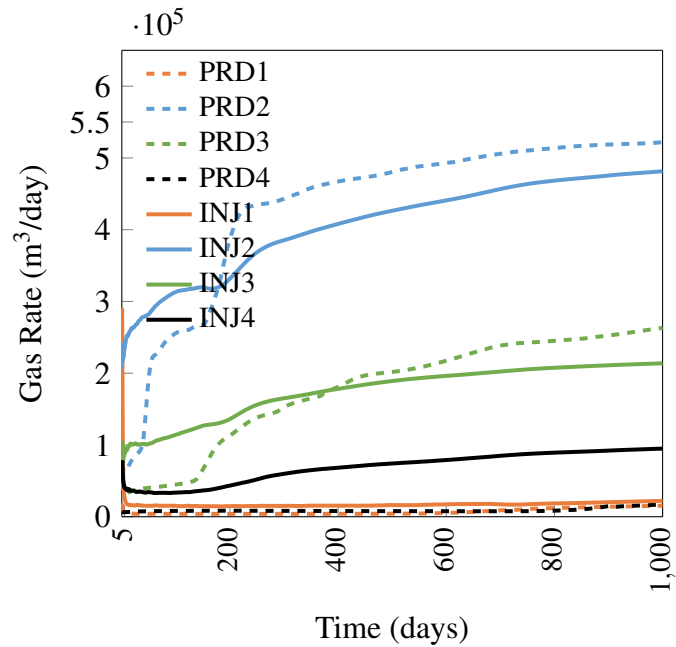


Figure 3.18: Gas rates in  $\text{m}^3/\text{d}$  for the injectors versus time for the reference case of Example 2.

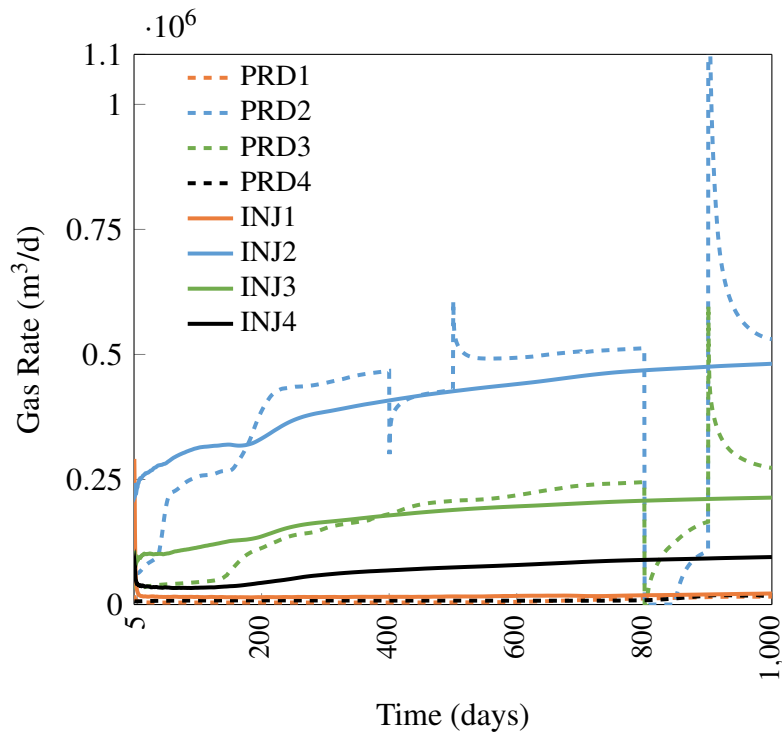


Figure 3.19: Gas rates in  $\text{m}^3/\text{d}$  for the injectors versus time for the optimal case of Example 2.

### 3.2.2 Optimization with geological continuation

Similarly to the previous example, we examine if the results can be further improved by using a continuation in geology. For this process we use ten different geologies, starting from the homogeneous version of the benchmark and gradually reaching the original geological values of the benchmark. In order to remain in the vicinity of the global optimum, we optimize sequentially the geologies until the final one. For this example, ten sequential optimizations have been made for all nine initial guesses. The controls from each optimized sub-geology are introduced as initial controls to the next geology. The geology variations are presented in Fig. 3.21. The objective values for each step of this continuation process are presented in Table 3.9. Also a visual representation of the depleted sub-reservoirs is shown at Fig. 3.22 where the gradual change of the oil saturation is depicted.

Step	$[p_I^a, p_P^a]$	$[p_I^l, p_P^l]$	$[p_I^u, p_P^u]$	$[p_I^l, p_P^a]$	$[p_I^l, p_P^l]$	$[p_I^l, p_P^u]$	$[p_I^u, p_P^a]$	$[p_I^u, p_P^l]$	$[p_I^u, p_P^u]$
0	56.23	56.08	56.45	55.74	56.13	56.07	56.08	56.08	56.1
1	59.24	59.31	57.38	59.33	57.45	59.31	59.23	59.31	59.23
2	60.2	60.43	59.65	60.67	59.07	60.43	60.43	60.43	60.28
3	59.36	59.67	59.04	60.3	58.91	59.67	59.67	59.67	59.67
4	57.7	58	57.72	58.57	57.44	58	58	58	58
5	56.08	56.34	56.09	56.68	55.76	56.34	56.34	56.34	56.34
6	54.63	54.87	54.45	55.07	54.67	54.87	54.87	54.87	54.87
7	53.36	53.54	53.34	53.47	53.32	53.54	53.54	53.54	53.55
8	52.19	52.3	52.19	52.22	51.35	52.3	51.85	52.3	52.3
9	51.36	51.44	51.36	51.43	51.35	51.44	51.44	51.44	51.44
10	51.07	51.14	51.04	51.11	51.07	51.14	51.13	51.13	51.13

Table 3.9: Cumulative oil production in  $10^3 \text{ m}^3$  for each geology step and all initial guesses (Example 2).

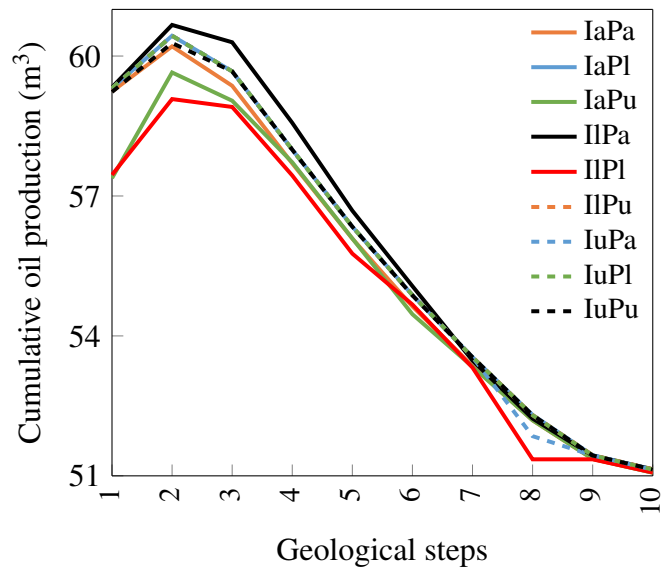


Figure 3.20: Cumulative oil production in  $\text{m}^3$  per geology step for nine initial guesses (Example 2).

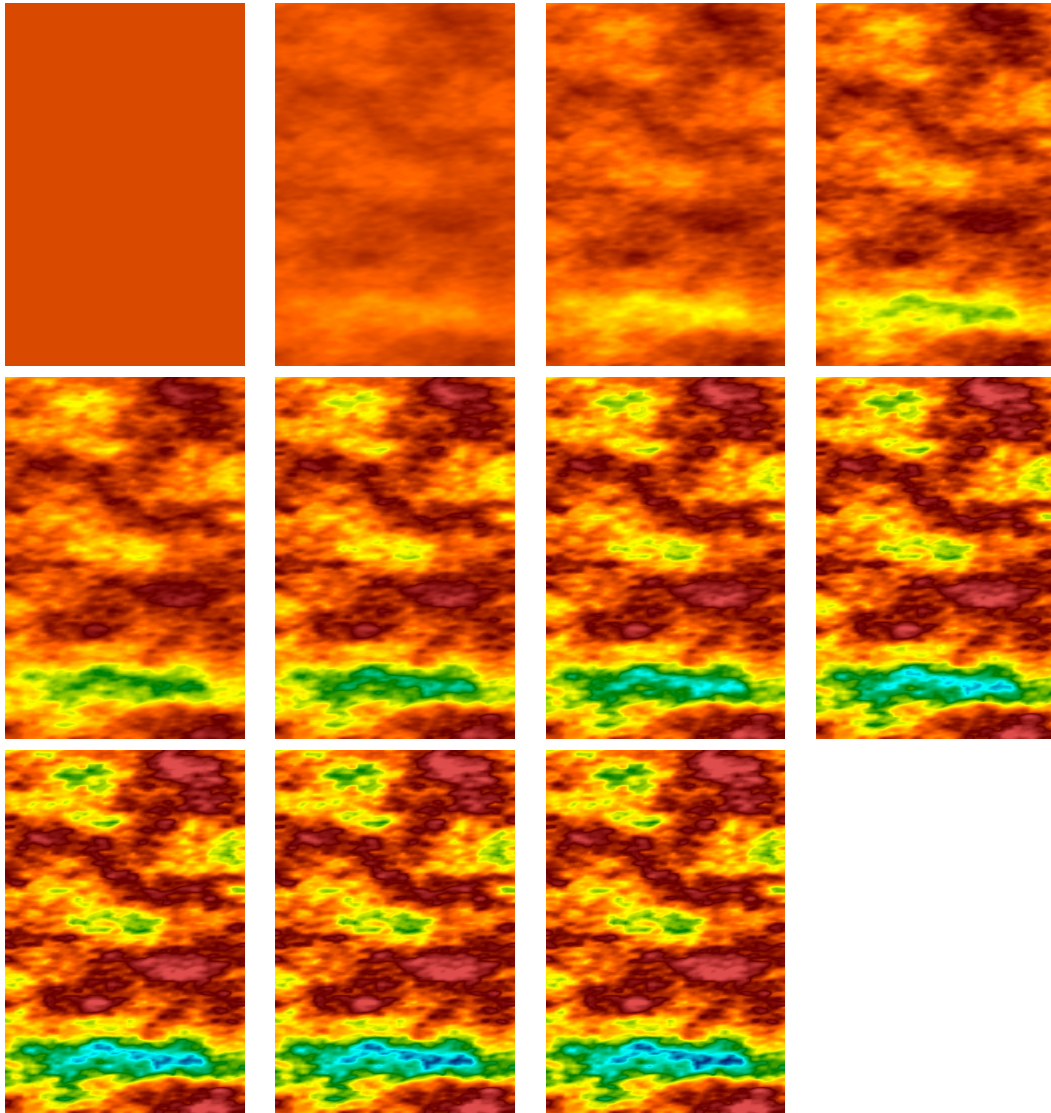


Figure 3.21: Permeability maps for all the geological steps used for optimization of cumulative oil in SPE10 top layer (Example 2).

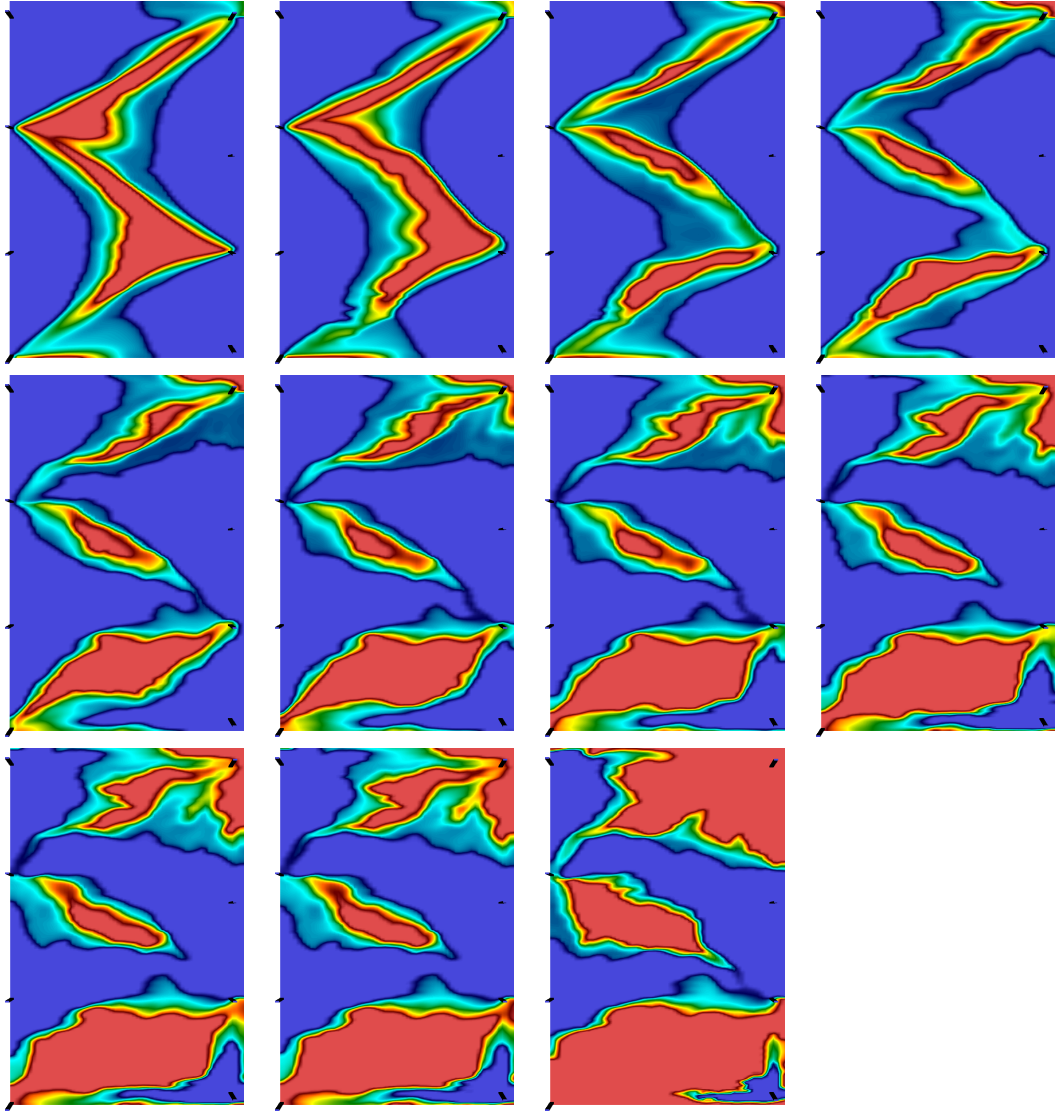


Figure 3.22: Oil saturation for the SPE10 top layer for all geological steps, starting from the homogeneous one (Example 2).

For this example, the geological continuation was examined for nine initial conditions. The cumulative oil for all methods and for all ten geology steps, are given in Table 3.10, in the respectively labeled columns. Similarly to the previous example, in order to evaluate the time discretization error, the final simulations were repeated for a smaller timestep. The results are presented in Table 3.10, in the columns labeled '*Ref\**', '*One\**' and '*Geo\**' respectively. The gradual change of the cumulative oil is presented in Fig. 3.20. The optimization process with the geological continuation resulted an improved optimum of  $51.5310^4$  m<sup>3</sup> instead of  $51.1910^4$  m<sup>3</sup> the one step optimization provides. A comparative representation of the results is presented in Fig. 3.23. Also, the BHPs, the oil and gas rates for the optimal result of geological continuation method are depicted in Fig. 3.24, 3.25, 3.26.

Run	Reference	<i>Ref*</i>	One step	<i>One*</i>	Continuation	<i>Geo*</i>
Reference	<b>50.86</b>					
$[p_I^a, p_P^a]$	38.87	38.83	51.18	51.17	51.07	51.08
$[p_I^a, p_P^l]$	45.79	45.77	51.19	51.18	51.14	51.15
$[p_I^a, p_P^u]$	29.2	29.17	51.19	51.18	51.04	51.04
$[p_I^l, p_P^a]$	28.84	28.85	51.01	50.99	51.11	51.08
$[p_I^l, p_P^l]$	38.31	38.32	51.18	51.17	51.07	51.08
$[p_I^l, p_P^u]$	28.25	28.31	50.91	50.88	51.14	51.16
$[p_I^u, p_P^a]$	46.29	46.19	51.19	51.18	51.13	51.14
$[p_I^u, p_P^l]$	50.91	<b>50.86</b>	51.2	<b>51.19</b>	51.13	<b>51.53</b>
$[p_I^u, p_P^u]$	39.68	39.57	51.19	51.18	51.13	50.9

Table 3.10: Oil production in  $10^4$  m<sup>3</sup> for nine initial guesses (Example 2). Results for simulation, optimization and geology steps. Optimal results shown in bold.

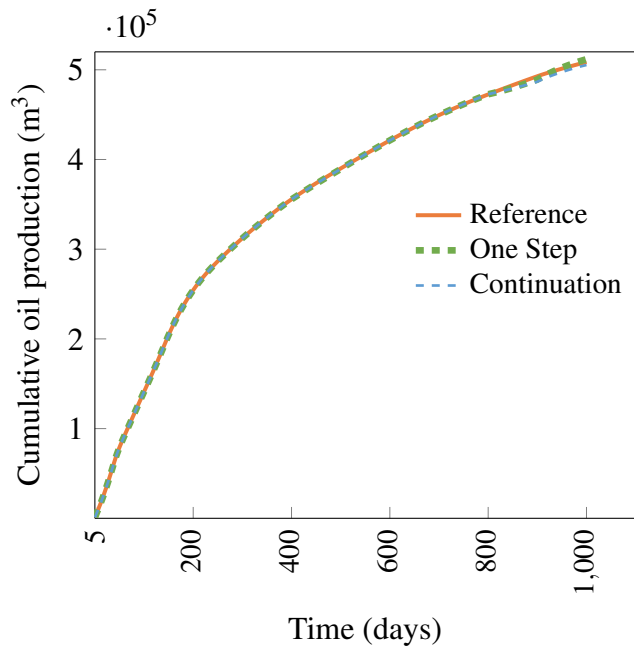


Figure 3.23: Cumulative oil production versus time for Example 2. Results are for reference case (orange curve), best optimized solution (green curve) and the geology continuation result (blue curve).

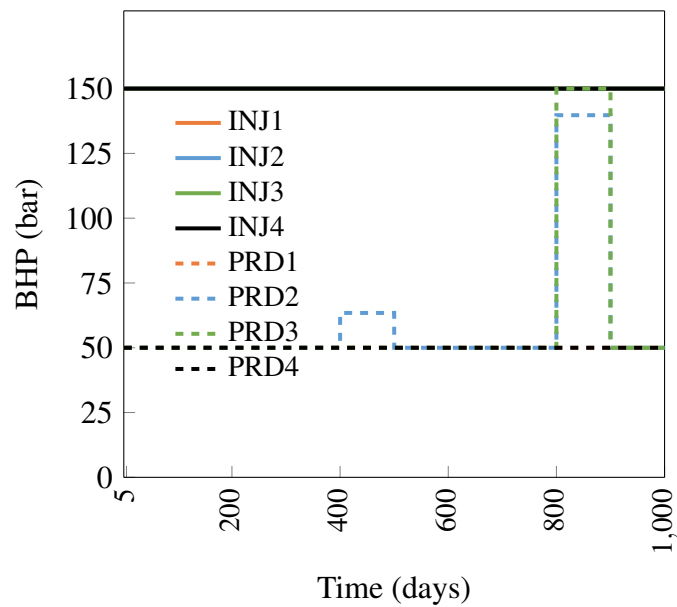


Figure 3.24: BHPs of injectors and producers versus time, for the optimal case of geology continuation of Example 2.

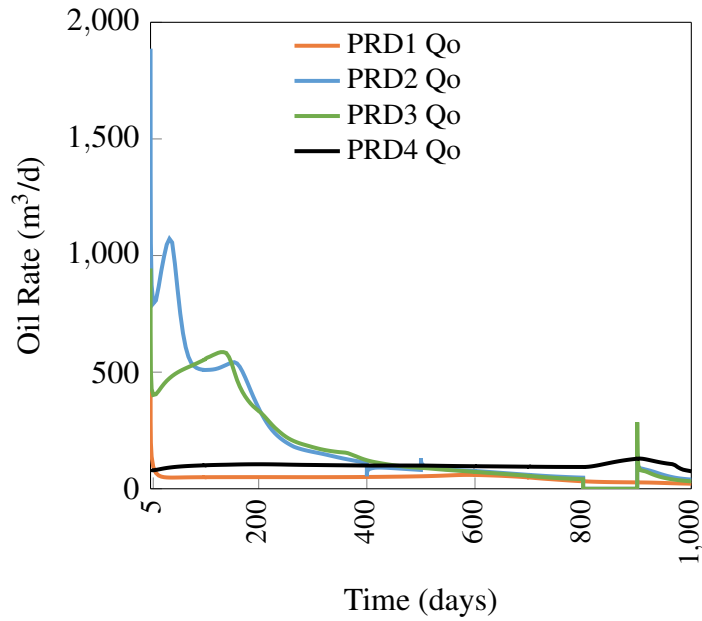


Figure 3.25: Oil rates in  $\text{m}^3/\text{d}$  of the producers versus time, for the optimal case of geology continuation of Example 2.

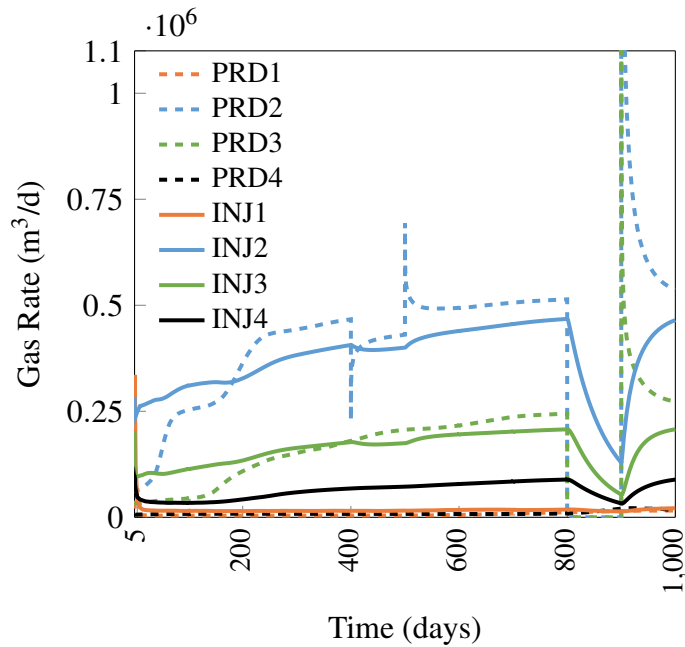


Figure 3.26: Gas rates in  $\text{m}^3/\text{d}$  for the injectors versus time, for the optimal case of geology continuation of Example 2.

### 3.2.3 Alternative objectives

Finally, we introduce two alternative objectives for production optimization: residual oil and residual of heavier component. All these objectives depend on the last state  $x_N$ . For the all the alternative objectives the equation (2.5), obtains the simplified form

$$J(\mathbf{x}, \mathbf{u}) = \varphi(\mathbf{x}_N), \quad (3.3)$$

and the Lagrange multipliers will satisfy the equations:

$$\frac{\partial \mathbf{g}_n^T}{\partial \mathbf{x}_n} \boldsymbol{\lambda}_n = - \frac{\partial \mathbf{g}_{n+1}^T}{\partial \mathbf{x}_n} \boldsymbol{\lambda}_{n+1}, \quad (3.4)$$

$$\frac{\partial \mathbf{g}_N^T}{\partial \mathbf{x}_N} \boldsymbol{\lambda}_N = - \frac{\partial \varphi_N^T}{\partial \mathbf{x}_N}. \quad (3.5)$$

The individual entries of  $\delta J_A / \delta \mathbf{u}$  are given by

$$\frac{\delta f_n}{\delta \mathbf{u}_n} = \boldsymbol{\lambda}_n^T \frac{\partial \mathbf{g}_n}{\partial \mathbf{u}_n}, \quad n = 1, 2, \dots, N. \quad (3.6)$$

The residual oil objective (3.7) expresses how much oil is left in the reservoir at the last time step. The function  $\varphi(\mathbf{x}_N)$  for this case takes the form

$$\varphi(\mathbf{x}_N) = \int_V S_o^N (1 - x_{\text{CO}_2}^N) \phi dV, \quad (3.7)$$

where  $\phi$  the porosity of the block, NB is the number of grid blocks, and  $S_o$  is the oil saturation of the block. We exclude the carbon dioxide  $\text{CO}_2$  because in the reservoir conditions of our benchmarks due to the particular reservoir temperature and pressure, it is usually dissolved in the liquid phase resulting an overestimation of the residual oil. The residual of heavier component (3.8), is a similar objective that is introduced to prioritise the removal of the heavier component, which is the least mobile component of the oil in place. For this case the function  $\varphi(\mathbf{x}_N)$  is written

$$\varphi(\mathbf{x}_N) = \int_V S_o^N x_{\text{C}_{10}^o}^N \phi dV, \quad (3.8)$$

where  $x_{\text{C}_{10}^o}$  is the molar fraction of the heavier component in the oil phase. From the volume integration in equations (3.7), (3.8) we exclude the grid cells fully saturated with the injected gas dissolved in the oil phase. In contrast to the cumulative oil that is maximised, each one of the aforementioned objective functions is minimized.

In Table 3.11 the reference solution results are given at column “*Ref*”, the one step optimization of cumulative oil at column “*One*”, the optimization of cumulative oil with the geological continuation approach at column “*Geo*”, the one step optimization of residual oil at column “*ROil*” and finally the one step optimization of the residual of heavier component at the column “*HeavC*”. The residual oil resulted in higher cumulative oil production compared to the reference essentially from every initial guess. On the contrary the residual of the heavier component did not outperformed the reference case.

Run	<i>Ref</i>	<i>One</i>	<i>Geo</i>	<i>ROil</i>	<i>HeavC</i>
$[p_I^a, p_P^a]$	38.83	51.17	51.08	50.85	50.63
$[p_I^a, p_P^l]$	45.77	51.18	51.15	50.82	50.71
$[p_I^a, p_P^u]$	29.17	51.18	51.04	50.85	50.68
$[p_I^l, p_P^a]$	28.85	50.99	51.08	50.97	50.51
$[p_I^l, p_P^l]$	38.32	51.17	51.08	50.95	50.64
$[p_I^l, p_P^u]$	28.31	50.88	51.16	<b>51.02</b>	50.67
$[p_I^u, p_P^a]$	46.19	51.18	51.14	50.9	50.64
$[p_I^u, p_P^l]$	<b>50.86</b>	<b>51.19</b>	<b>51.53</b>	50.94	<b>50.86</b>
$[p_I^u, p_P^u]$	39.57	51.18	50.9	50.95	50.68

Table 3.11: Oil production in  $10^4 \text{ m}^3$  for nine initial guesses (Example 2). Results for simulation, optimization and geology steps. Optimal results shown in bold.

### 3.3 Concluding remarks

In this work we formulated and tested an adjoint-based optimization procedure for compositional reservoir simulation adopting a continuation approach with respect to the geology. Numerical results were presented for two example cases of increasing complexity. Nine runs, starting from different initial conditions, were performed in all cases, using box-constraints on the control variables. In our examples, the control variables were the time-varying well BHPs. In the simplest case (Example 1), the optimization of cumulative oil using continuation increased the oil production by 2.6%. For the second benchmark problem (Example 2), the optimization of cumulative oil using continuation produced results that were essentially the same up to the discretization errors with respect to space and time variables from all nine initial guesses. The re-evaluation of the optimal objectives with a much smaller time step size, revealed that one of the optimal solutions using continuation increased by 0.8% providing an overall increase of the oil production over the reference case of 1.3%. This result strongly suggests that first order time discretization, as the backward Euler adopted in this work, may be inadequate to capture small scale transient phenomena, and thus higher order time discretization methods may be more effective.

There are a number of areas in which future research should be directed. The present methods should be also tested with nonlinear constraints such as maximum gas injection and/or production rates specified at each injector and/or producer well. We anticipate that the continuation with respect to the geology, will assist production optimization problems subject to nonlinear inequality constraints, since the starting point of the optimization will always be a feasible solution, once the feasibility has been achieved in the homogeneous reservoir. Finally it is of interest to apply the continuation framework to larger and more realistic 3D reservoir models where gravity effects add another level of difficulty giving room to the optimizer to dictate solutions that increase the oil production even further than the one observed in our 2D benchmarks.

## **Acknowledgements**

Firstly, I would like to express my deepest appreciation to my supervisor Dr. Drosos Kourounis for his continuous support, his patient guidance and immense knowledge. I am also indebted to Professor Olaf Schenk for his provided expertise that greatly assisted the research. I gratefully acknowledge the support and generosity of the Università della Svizzera italiana for sponsoring the Masters Research Scholarship (MaRS) program, without which the present thesis could not have been completed. In addition, a special word of gratitude is due to all my professors in Petroleum Engineering department of Technical University of Crete for their guidance and their valuable advice that inspired me to pursue a career in the petroleum industry. I would also like to extend my thanks to my colleagues for the academic year 2015/2016 for their social and professional support. Last but not least, I would like to thank my family and my husband for their extraordinary support.



# Bibliography

- Anazi, B. D. A. (2007). Enhanced oil recovery techniques and nitrogen injection. CSEG Recorder, pages 29–33.
- Asheim, H. (1988). Maximization of water sweep efficiency by controlling production and injection rates. In SPE Paper 18365 presented at the SPE European Petroleum Conference, London, UK.
- Aziz, K. and Settari, A. (1979). Petroleum Reservoir Simulation. Applied Science Publishers, London.
- Bonnans, Fredaric, J., Gilbert, Charles, J., Lemarachal, Sagastizabal, C., and A., C. (2006). Numerical optimization: Theoretical and practical aspects. Universitext, Berlin: Springer-Verlag.
- Brouwer, D. R. and Jansen, J. D. (2004). Dynamic optimization of water flooding with smart wells using optimal control theory. SPE Journal, 9(4):391–402.
- Bryson, A. and Ho, Y. (2001). Applied Optimal Control. Taylor and Francis (Hemisphere), Levittown.
- Cao, H. (2002). Development of techniques for general purpose simulators. Ph.D. thesis, Stanford University.
- Chavent, G., Dupuy, M., and Lemonnier, P. (1975). History matching by use of optimal control theory. SPE Journal, 15:74–86.
- Chen, W., Gavalas, G., and Wasserman, M. (1974). A new algorithm for automatic history matching. SPE Journal, 14(6):593–608.
- Christie, M. and Blunt, M. (2001). Tenth SPE comparative solution project: a comparison of upscaling techniques. SPE Reservoir Evaluation and Engineering, 4(4):308–317.
- Coats, K. (1980). An equation of state compositional model. SPE Journal, 20(5):363–376.

- Echeverría Ciaurri, D., Isebor, O. J., and Durlofsky, L. J. (2011). Application of derivative-free methodologies to generally constrained oil production optimisation problems. International Journal of Mathematical Modelling and Numerical Optimisation, 2:134–161.
- et al., S. K. R. (2011). Surface and subsurface requirements for successful implementation of offshore chemical enhanced oil recovery.
- et al., T. A. J. (2010). Comparative study of different eor methods.
- Fleshman, R. and Lekic, O. (1999). Artificial lift for high volume production. Oilfield Review, (11):48–63.
- Gill, P. E., Murray, W., and Saunders, M. A. (2005). SNOPT: An SQP algorithm for large-scale constrained optimization. SIAM Rev., 47(1):99–131.
- Glover, P. (2001). Formation Evaluation MSc Course Notes. Aberdeen University.
- Gunzburger, M. (2003). Perspectives in Flow Control and Optimization. SIAM.
- Hager, W. W. (2000). Runge-Kutta methods in optimal control and the transformed adjoint system. Numerische Mathematik, 87(2):247–282.
- Han, C., Wallis, J., Sarma, P., Li, G., Schrader, M. L., and Chen, W. (2013). Adaptation of the CPR preconditioner for efficient solution of the adjoint equation. SPE Journal, 18(2):207–213.
- Jansen, J. D. (2011). Adjoint-based optimization of multi-phase flow through porous media - a review. Computers & Fluids, 46(1):40 – 51.
- Juttner, I. (1997). Oil displacement in miscible condition. Rudarsko-GeoloÅąko-NAFTNI Zbornik, 9(1):63–66.
- Kermen, E. (2011). Thermal Enhancement of Water-Flooding in Medium- Heavy Oil Recovery, in Applied Earth Sciences. Delft University of Technology, The Netherlands.
- Kourounis, D., Durlofsky, L. J., Jansen, J. D., and Aziz, K. (2014). Adjoint formulation and constraint handling for gradient-based optimization of compositional reservoir flow. Computational Geosciences, pages 1–21.
- Kourounis, D. and Schenk, O. (2015). Constraint handling for gradient-based optimization of compositional reservoir flow. Computational Geosciences, 19(5):1109–1122.
- Kulkarni, M. M. (2003). Immiscible and Miscible Gas-Oil Displacements in Porous Media. Louisiana State University.

- Li, R., Reynolds, A., and Oliver, D. (2003). History matching of three-phase flow production data. SPE Journal, 8(4):328–340.
- Liu, W., Ramirez, W., and Qi, Y. (1993). Optimal control of steam flooding. SPE Advanced Technology Series, 1(2):73–82.
- Mattax and Dalton (1990). Reservoir simulation. Society of Petroleum Engineers.
- Mehos, G. and Ramirez, W. (1989). Use of optimal control theory to optimize carbon dioxide miscible-flooding enhanced oil recovery. Journal of Petroleum Science and Engineering, 2(4):247–260.
- Melzer, L. S. and Midland, T. (2012). Carbon dioxide enhanced oil recovery (CO<sub>2</sub>-EOR): Factors involved in adding carbon capture, utilization and storage (CCUS) to enhanced oil recovery.
- Meyer, J. P. (2007). Summary of carbon dioxide enhanced oil recovery (CO<sub>2</sub>-EOR) injection well technology. American Petroleum Institute, page 54.
- Nadarajah, S. and Jameson, A. (2000). A comparison of the continuous and discrete adjoint approach to automatic aerodynamic optimization. In AIAA 38th Aerospace Sciences Meeting and Exhibit, Reno, NV.
- Oliver, D., Reynolds, A., and Liu, N. (2008). Inverse Theory for Petroleum Reservoir Characterization and History Matching. Cambridge University Press, Cambridge.
- Petra, N. and Stadler, G. (2011). Model variational inverse problems governed by partial differential equations. ICES Report 11-05, The Institute for Computational Engineering and Sciences, The University of Texas at Austin.
- Ramirez, W. (1987). Application of Optimal Control Theory to Enhanced Oil Recovery. Elsevier Science Ltd, Amsterdam.
- Romero-Zeran, L. (2012). Advances in Enhanced Oil Recovery Processes. University of New Brunswick, Canada.
- Sarma, P., Durlofsky, L. J., Aziz, K., and Chen, W. H. (2006). Efficient real-time reservoir management using adjoint-based optimal control and model updating. Computational Geosciences, 10(1):3–36.
- Shine, J. and Holtz, M. (2008). Reserve growth & higher recovery using nitrogen gas injection. Proc. 2008 Wyoming EOR/IOE Conference.
- Stengel, R. (1986). Stochastic Optimal Control Theory and Application. Wiley, New York.

- Sudaryanto, B. and Yortsos, Y. (2000). Optimization of fluid front dynamics in porous media using rate control. Physics of Fluids, 12(7):1656–1670.
- Syed, F. I., Tunio, A. H., and Ghirano, N. A. (2011). Compositional analysis and screening for enhanced oil recovery processes in different reservoir and operating conditions. International Journal of Applied, 1(4).
- Virnovski, G. (1991). Waterflooding strategy design using optimal control theory. In 6th European IOR Symposium, pages 437–446, Stavanger, Norway.
- Voskov, D. and Tchelepi, H. (2012). Comparison of nonlinear formulations for two-phase multi-component EoS based simulation. Journal of Petroleum Science and Engineering, 82–83:101–111.
- Voskov, D. V., Younis, R., and Tchelepi, H. A. (2009). Comparison of nonlinear formulations for isothermal compositional flow simulation. In SPE paper 118966 presented at the SPE Reservoir Simulation Symposium, The Woodlands, Texas, USA.
- Walther, A. (2007). Automatic differentiation of explicit Runge-Kutta methods for optimal control. Computational Optimization and Applications, 36(1):83–108.
- Young, L. and Stephenson, R. (1983). A generalized compositional approach for reservoir simulation. Journal of Petroleum Science and Engineering, 23(5):727–742.
- Younis, R. and Aziz, K. (2007). Parallel automatically differentiable data-types for next-generation simulator development. In SPE Paper 106493 presented at the SPE Reservoir Simulation Symposium, Houston, Texas.
- Younis, R., Tchelepi, H., and Aziz, K. (2010). Adaptively localized continuation-Newton method–Nonlinear solvers that converge all the time. SPE Journal, 15(2):526–544. SPE-119147-PA.